Pysarenko, L., Savenets, M., & Pishniak, D. (2025). Linking weather variability and climatic pressure dipole in the Antarctic region of Amundsen — Bellingshausen — Weddell Seas.
Ukrainian Antarctic Journal, *23*(2), 3—29.
https://doi.org/10.33275/1727-7485.2.2025.748

Гідрометеорологічні та океанографічні дослідження

Hydro-Meteorological and Oceanographic Research

Linking weather variability and climatic pressure dipole in the Antarctic region of Amundsen — Bellingshausen — Weddell Seas

Larysa Pysarenko [1, 2, *], **Mykhailo Savenets** [1], **Denys Pishniak** [2]

[1] Ukrainian Hydrometeorological Institute of the State Emergency Service of Ukraine and the National Academy of Sciences of Ukraine, Kyiv, 03028, Ukraine
[2] State Institution National Antarctic Scientific Center of the Ministry of Education and Science of Ukraine, Kyiv, 01601, Ukraine

*** Corresponding author:** lolinal@ukr.net, larpys@uhmi.org.ua

Abstract. The climatic pressure dipole, formed by the Amundsen Sea Low (ASL) and the high-pressure area east of the Antarctic Peninsula (AP), is a major contributor to weather variability in West Antarctica and the peninsula region. Under the ongoing climate change, the role of this pressure configuration often remains uncertain. Using ERA5 reanalysis data for 1991—2022, we investigated the response of precipitation types and near-surface meteorological fields to variability in the climatic pressure dipole. A deepening eastward shift of the ASL increased snowfall over the Amundsen and Bellingshausen Seas, particularly near the low-pressure center itself, while precipitation near the AP tended to shift from solid to mixed or liquid phases. Strengthening of high pressure over the western Weddell Sea — especially when displaced closer to the AP — led to an overall decrease in precipitation, but with more frequent freezing rains and ice pellets over the northeastern AP. These relationships, however, were highly heterogeneous and exhibited strong seasonal features. Near-surface meteorological parameters showed weaker responses to the pressure dipole than precipitation. A deepened ASL generally lowered air temperature and saturation point over the eastern Bellingshausen Sea, while its eastward displacement produced warmer conditions across the study area. A high-pressure ridge east of the AP strongly influenced the thermal regime over the Weddell Sea and Dronning Maud Land, and was associated with intensified southerly and westerly winds in the southern part of the AP. Overall, this study enhances understanding of how surface meteorological conditions generally respond to atmospheric pressure variability in the region.

Keywords: Amundsen Sea Low, Antarctica, atmospheric pressure, meteorological variables, precipitation, reanalysis

1 Introduction

Manifestations of climate change have become increasingly evident in Antarctica, the coldest continent (Wang et al., 2025), including the adjacent waters of the Southern Ocean (Cai et al., 2023). While economic activity in this region is subject to strict regulation (Hughes et al., 2021; Press & Constable, 2022), the global temperature increase reflects a cause-and-effect relationship driven by the long-lasting footprint of greenhouse gases (IPCC, 2022).

The marine Antarctic region remains highly vulnerable (Boothroyd et al., 2024), with pronounced changes in meteorological conditions (Naakka et al., 2021; Wang et al., 2025), particularly near the Antarctic Peninsula (AP) (Siegert et al., 2019). Recent studies have identified significant positive air temperature trends, temporarily interrupted by a short pause (Carrasco et al., 2021); variability in precipitation (Vignon et al., 2021), including extreme events (Pysarenko et al., 2023); changes in ice mass balance (Shepherd et al., 2018), posing risks of a significant sea-level rise (Li et al., 2024); alterations in ice-shelf dynamics (Worster, 2014); and other changes.

Numerous ocean—land—atmosphere interactions (Ayres et al., 2022) and regional circulation variability (Schlosser et al., 2011; Hepworth et al., 2024) play important roles in driving current changes in the maritime Antarctic region. Two stable pressure patterns strongly influence the weather near the AP and West Antarctica: the Amundsen Sea Low (ASL) (Raphael et al., 2016) — climatological prevailing low-pressure area; and the relatively high-pressure zone along the AP over the western Weddell Sea — formed as a result of air subsidence and atmosphere-ice interactions and amplified by orography (Turner et al., 2002; Zhang et al., 2021; Ayres et al., 2024). In the current paper, we use the term “climatic pressure dipole” to refer to these two prevailing pressure areas. The Weddell Sea Low (Zhang et al., 2021) is farther away and has a weaker impact on weather patterns west of the AP. The current pace of global warming is expected to intensify the ASL (Gao et al., 2021; Dalaiden et al., 2024), while distinct seasonal changes are associated with the so-called “Foehn phenomenon” in the western Weddell Sea (Orr et al., 2008; Andres-Martin et al., 2024).

This study continues our previous work (Pysarenko et al., 2023), which examined the relationships between pressure parameters in the Amundsen and Bellingshausen Seas and precipitation totals, including extremes above the 95th percentile. That study showed that the location and shifts of ASL significantly affect precipitation over West Antarctica and the AP. The deepening of the ASL may lead to decreased precipitation over the Getz Ice Shelf and increased precipitation over the western AP. The results were obtained using ERA5 reanalysis data, which is among the most accessible and reliable datasets for the Antarctic region that includes assimilation of observational data to investigate causal relationships between pressure parameters and other meteorological elements.

However, previous studies highlighted the need to enlarge the study domain to include not only the Amundsen and Bellingshausen Seas and adjacent ice basins, but also the Weddell Sea and surrounding regions. Furthermore, a deeper analysis would require incorporating additional variables and precipitation types. The aim of this research is to investigate the spatio-temporal patterns of meteorological variables and precipitation types in response to the climatic pressure dipole, particularly the interaction between the ASL and the climatological high-pressure region over the Weddell Sea. This work seeks to advance understanding of atmospheric processes in the Antarctic region, still relatively understudied due to limited observational data.

The study starts by analysing the general climatological distribution of pressure parameters and other meteorological variables over the study domain. It then focuses on the impact of the climatic pressure dipole on meteorological conditions, particularly certain precipitation types.

2 Data and methodology

The study is a logical extension of previous research (Pysarenko et al., 2023), which focused on the dependencies of the total extreme precipitation patterns on ASL. To obtain more comprehensive estimates, we expanded the study domain and increased the sets of pressure parameters and the dependent variables.

Since meteorological fields in the region are influenced not only by the ASL (a relatively low-pressure area) but also by persistent high-pressure patterns over the Weddell Sea, the study area was significantly enlarged (Fig. 1). Overall, the area of interest extends from 160°W to 20°E longitude and, as in the previous research, has the latitudinal range from 62°S to 82°S. Within this domain, we searched the area with the prevailing low pres-

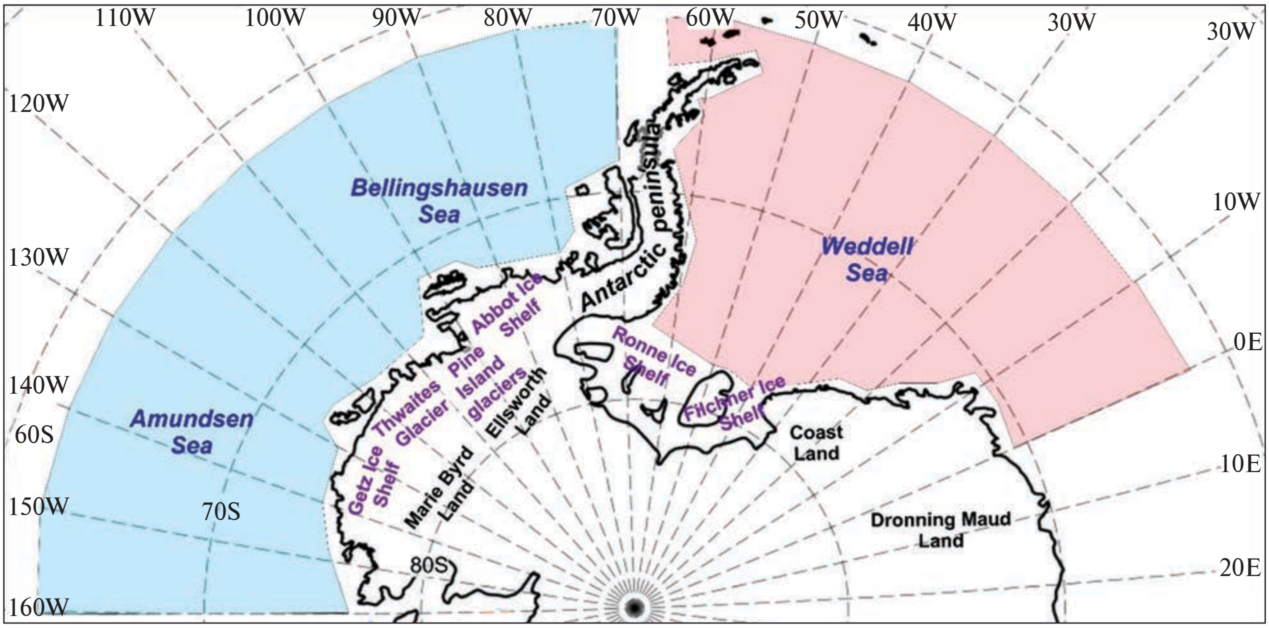

Figure 1. Study domain including two areas: with prevailing low (blue) and high pressure (red)

sure over the territory shown in blue in Figure 1, with the high pressure in the area shown in red.

The following pressure parameters were used to analyse cause—effect relationships with meteorological characteristics: (1) the minimum pressure over Bellingshausen or Amundsen Seas; (2) the maximum pressure over Weddell Sea or adjacent areas (see the red area in Fig. 1); (3) longitude of the minimum pressure; (4) longitude of the maximum pressure; (5) distance between the centers of the minimum and maximum pressures; (6) spatial gradient between the centers of minimum and maximum pressures; (7) distance from each grid point in the study area to the center of minimum pressure; (8) distance from each grid point in the study area to the center of maximum pressure. For the calculations, longitudes were considered as negative for western longitudes and positive for eastern longitudes. If the central pressure was outside this large domain, the computations used the extremum at the edge of the domain. Distances between grid cells and pressure centers were calculated using the haversine formula (see details in Pysarenko et al., 2023).

The meteorological characteristics analysed for spatial correlations with the pressure parameters were: (1) 2-m air temperature; (2) 2-m dew point; (3) the *u*-component of 10-m wind; (4) the *v*-component of 10-m wind; (5) total precipitation; (6) frequency of specific precipitation types at the surface — snow, wet snow (i.e., snow particles which are starting to melt), rain, freezing rain (i.e., supercooled raindrops which freeze on contact with the ground and other surfaces), snow pellets, mixed precipitation, and no precipitation. The precipitation phase in ERA5 is given as instantaneous values representing the dominant type at the model time step of 12-minute interval (ECMWF, 2025a). To determine precipitation types in ERA5, rain and snow have been represented as separate prognostic variables, while other types are diagnosed from the profiles of rain and snow combined with near-surface temperature from the model (ECMWF, 2025b). In particular, positive air temperature in the lower atmosphere for rain and negative for snow; a melting layer in the lower atmosphere with a small amount (<20%) of liquid water for wet snow; and for the mixed type (snow with 20—

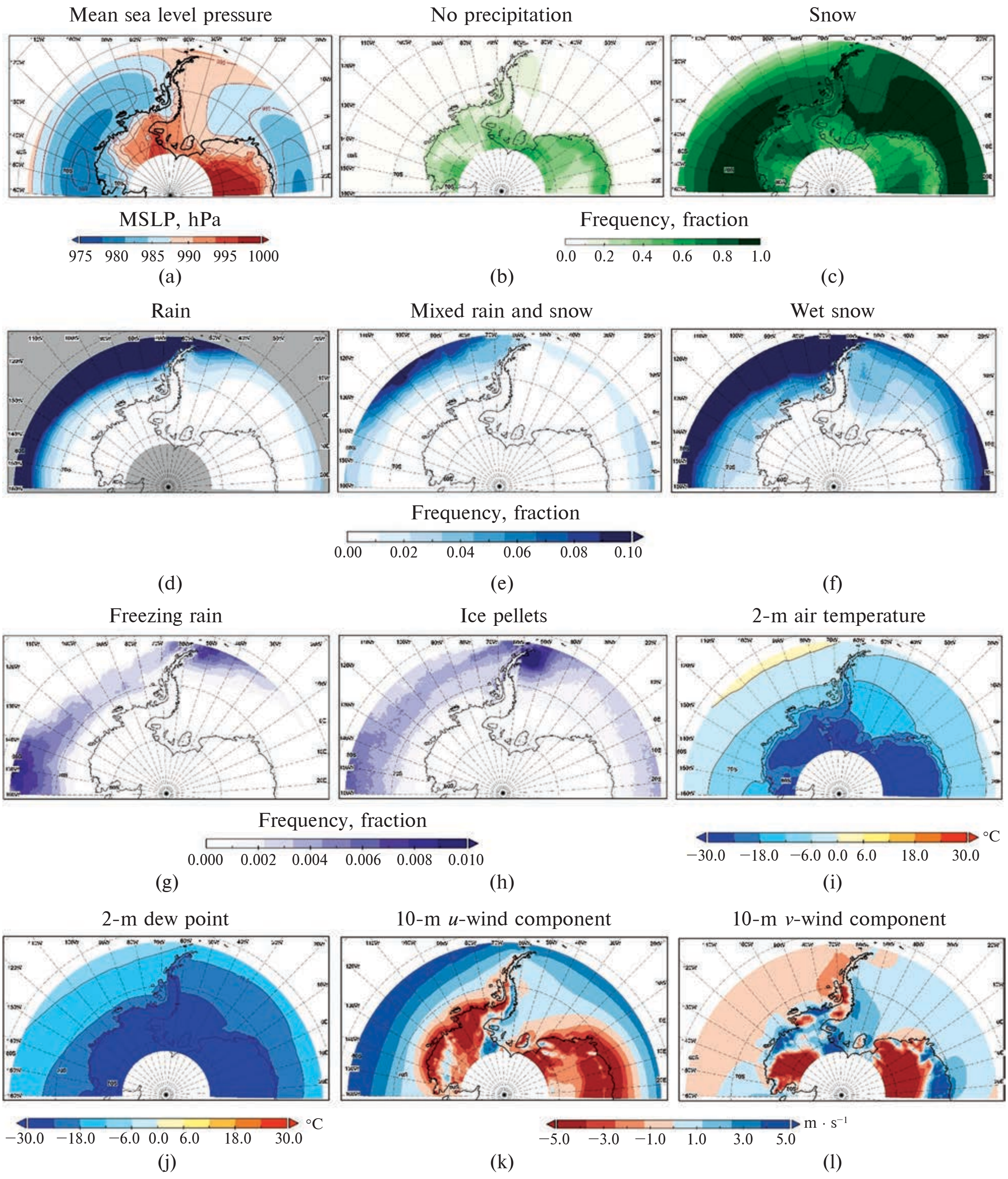

Figure 2. Multi-year (1991–2022) mean fields over the region of study for mean sea level pressure (a), no precipitation (b), snow (c), rain (d), mixed rain & snow (e), wet snow (f), freezing rain (g), and ice pellets (h), 2-m air temperature (i), 2-m dew-point (j), 10-m *u*- (k) and *v*- (l) wind components

80% liquid water), the melting layer intercepted the ground (ECMWF, 2025b). Ice pellets appear if there is a warm layer above a near-surface sub-zero layer: the snow aloft is only partially melted in the warm layer (20–80% snow at its base) and re-freezes in the underlying cold air (ECMWF, 2025b). For freezing rain, the conditions are similar, but the snow is almost entirely melted in the warm layer (ECMWF, 2025b). The frequency of precipitation types was calculated for each month as the number of time steps with phenomena divided by the total number of time steps.

Source data for 1991–2022 were taken from the ERA5 reanalysis (Hersbach et al., 2023) with hourly values at a 0.25° × 0.25° horizontal resolution for the study domain, retrieved from the Climate Data Store (CDS, https://cds.climate.copernicus.eu/datasets/reanalysis-era5-single-levels?tab=overview, accessed 15.08.2025). As noted in Pysarenko et al. (2023), *in-situ* observations in Antarctica are scarce and point-like; therefore, modelling and data assimilation uncertainties can influence the atmosphere–ocean–land interactions and should be taken into account during results analysis and interpretation. While ERA5, in general, showed accurate results for the Antarctic Peninsula region (Tetzner et al., 2019), it has known biases in precipitation (Roussel et al., 2020; Vignon et al., 2021). These biases include underestimation of rain occurrences (Vignon et al., 2021) and a positive bias of up to 30 mm · year^{-1} for precipitation over complex terrain (Roussel et al., 2020).

The analysis was performed on monthly data derived from the hourly values. For most meteorological variables, monthly averages were calculated; for precipitation and its types, monthly accumulated values were used. The frequency of each precipitation type was computed as the fraction of time steps in which it occurred at a given grid cell. As in our previous research, we used the Spearman rank correlation coefficient (95% confidence level). It is more suitable for the data than the Pearson correlation coefficient, as the latter assumes that the time series are approximately normally distributed. All the relationships were investigated both as a whole multiannual period and broken down by season: austral winter, spring, summer, and autumn.

3 Results

3.1 Basic characteristics of the pressure parameters in the region

The typical mean sea level pressure (MSLP) field in the study region is clearly divided by the AP. To the west, lower pressure dominates, covering the Bellingshausen and Amundsen Seas, with multi-year averages below 980 hPa (see Fig. 2a). In contrast, higher MSLP values, around 990 hPa, are observed over the Weddell Sea east of the AP. This high-pressure area is narrower than the low-pressure region and is mostly confined to the area up to 40°W. Beyond this, another zone of low pressure is observed.

The multi-year average position of the lowest-pressure center (976 hPa) is located at 70°S 136°W. The highest-pressure center (994 hPa) is at 67°S 50°W. The positions of these two baric extremums, 2935 km apart, result in an average pressure gradient of 6.42 hPa per 1000 km.

The pressure minimum (corresponding to the ASL) generally ranged from 970 to 985 hPa (see Fig. A1a). The most extreme monthly MSLP values were observed in 1991–1994 and 2007 (over 990 hPa), and in 1998, 2008, 2011, and 2016, dropping as low as 960 hPa. The maximum pressure typically ranged between 990 and 1000 hPa. The highest monthly values exceeded 1005 hPa in 1995, 2000, 2009, 2011, and 2016, while the lowest fell below 985 hPa in 1998, 2000, 2001, 2006, 2008, 2012–2014, 2018, and 2022. As shown, in certain months the pressure extremes can be atypical – for example, the ASL, usually a low-pressure pattern, may exhibit unusually high pressure, while the Weddell Sea, typically a high-pressure area, may show lower values. Nevertheless, there were no months with a reversed pressure distribution: even at the highest MSLP in the ASL region, the pressure over the Weddell Sea remained higher.

The longitude of the elements of the climatic pressure dipole pinpoints their position and is a key factor influencing the pressure gradient across the region. The position of the pressure minimum is more variable than that of the maximum pressure east of the AP (see Fig. A1b). This is expected, as the ASL represents a climatological pressure pattern, whereas the high-pressure area over the Weddell Sea results from ice-atmospheric feedbacks (Ayres et al., 2024) and is amplified in its western part by orographic influence of the AP on atmospheric circulation (Turner et al., 2002; Zhang et al., 2021). The ASL is rarely located east of 80°W and occasionally shifts to the western edge of the study domain, indicating that the actual pressure minimum may lie even farther west. In contrast, the high pressure over the Weddell Sea is often near the eastern coast of the AP and is geographically constrained by land. In certain months, its easternmost position can reach as far as 0°E.

The distance between high- and low-pressure patterns is crucial for determining pressure gradients and the frequency of warm air mass transport toward the Antarctic coast. Monthly values of this distance range from 1000 to 5000 km (see Fig. A1c), with the majority falling within the 2500—3500 km interval. Spatial pressure gradients can vary from 2 hPa to over 12 hPa per 1000 km (see Fig. A1d). Notably, the pressure gradient is negatively correlated with the distance between pressure centers (correlation coefficient: −0.50). The correlation with the pressure minimum within ASL is −0.45, while the correlation with the maximum pressure over the Weddell Sea is only 0.24. This indicates that the ASL plays a more significant role in generating stronger pressure gradients.

There are no statistically significant trends in most pressure parameters (see Fig. A1). There were slight downward trends in the minimum and maximum pressures (see Fig. A1a). The magnitude of these trends is 0.9—1.5 hPa per decade.

3.2 General spatial distribution of the meteorological variables

The study region is characterised by a predominantly meridional gradient of meteorological parameters over marine areas, interrupted by the Antarctic coast and the influence of orography. On average, the area to the west of the AP was warmer than the area to the east. The −10 °C isoline followed the Antarctic coastline from the west up to the AP (Fig. 2i), but extended over the marine areas of the Weddell Sea, located slightly north of 70°S, to the east of the AP. Similar spatial patterns were observed for the dew-point temperature, with the −20 °C isoline following the coast from the west to the AP, and over marine areas to the east (Fig. 2j). The influence of orography on air temperature distribution is clearly visible in Figure 2i, j.

A significant westerly wind was observed from the north to about 70°S over the Amundsen and Bellingshausen Seas (Fig. 2i), where the average *u*-component of wind exceeded 2 m $\cdot$ s^{-1}. Over the Weddell Sea, westerly winds were less pronounced. Most coastal areas experienced strong easterly winds, with the *u*-component reaching −4 m $\cdot$ s^{-1}. The role of the AP mountain ridge is evident, with opposite *u*-component wind directions on its western and eastern sides. The western part of the study domain (to the west of the AP) is characterised by prevailing northern winds (negative *v*-component), while southern winds are more typical to the east of the AP (Fig. 2j). However, these prevailing wind differences are relatively small, mostly within ±1 m $\cdot$ s^{-1}. The highest wind-component values were observed over certain parts of the continent and its coastal areas (Fig. 2i, j).

Marine areas of Antarctica within the study domain are characterised by a high frequency of precipitation, in contrast to the interior continental regions. Figure 2 shows the frequencies of different precipitation types (Fig. 2c—h) as well as the frequency of no-precipitation periods (Fig. 2b). At each grid point, the sum of the fractional values from the presented maps equals 1.0 (or 100%). Over marine areas, precipitation occurs more than 80% of the time. Due to the orographic effect of the AP, the region to the east is somewhat drier, with the frequency of no-precipitation cases reaching about 30% (Fig. 2b).

Snow is the dominant precipitation type. Its spatial distribution has a typical zonal pattern. In most marine areas near Antarctica, the frequency of snow exceeds 75%. It must be considered that the observed snowfall frequency might be slightly overestimated by the ERA5 datasets in Antarctica (Hellmuth et al., 2025). It decreases notably near the coast, except in the northern part of the AP. Apart from snow, three other precipitation types can reach a frequency of up to 0.1 in certain parts of the study domain – rain, mixed rain and snow, and wet snow (Fig. 2d–f). Wet snow is observed furthest south, while rain is less frequent in these southern regions. As with other meteorological variables, the AP significantly influences the spatial distribution of precipitation types. Overall, the Weddell Sea exhibits weaker zonal precipitation patterns, largely due to the orographic impact of the AP on air masses.

Freezing rain and ice pellets are rare, with maximum frequencies of about 1% (Fig. 2g, h). Two regions within the study domain exhibit local maxima for these types. Their highest probability is near the eastern coast of the AP, illustrating its strong orographic effects. They are also more frequent in the northwestern part of the study domain, relatively far from Antarctica.

3.3 Dependence of meteorological variables on the pressure extrema

3.3.1 Impact of pressure parameters on precipitation and its specific types

Precipitation totals

Some aspects of the influence of pressure characteristics on total precipitation were presented in our previous research (Pysarenko et al., 2023). The current paper focuses on additional pressure drivers, such as the high-pressure area in the western Weddell Sea and its distance and spatial pressure gradient to the ASL.

The highest central pressure results in negative correlations with total precipitation up to –0.5 that are typical over the Weddell Sea, whereas positive correlations are observed along Getz Ice Shelf, Thwaites Glacier, and adjacent marine areas of the Amundsen Sea, annually (Fig. 3a). Seasonally, negative relationships of about –0.4 to –0.6 expand to cover the northern part of the AP and the adjacent marine area of the Bellingshausen Sea (Fig. 3e) in winter and the northern part of the Weddell Sea (Fig. 3f) in spring; the impact decreases markedly during the summer (Fig. 3g). In autumn, there are the most significant statistical relationships and contrasts between the abovementioned regions (Fig. 3h): negative correlations over the Weddell Sea and positive (up to 0.7) over the Getz Ice Shelf and Thwaites Glacier. In general, the strengthening high-pressure center over the Weddell Sea leads to a decrease in precipitation in this region. Over the southern part of the Amundsen Sea and the Getz Ice Shelf, the relationship between total precipitation and high pressure is direct and unexpectedly strong, representing a noticeable teleconnection between separate atmospheric processes. In contrast to the value of high pressure, its longitude contributes to all seasonal and annual values. Yearly precipitation totals respond positively to the longitude of high pressure over the eastern part of the AP (correlation up to 0.4) and negatively along the coastal areas over the Getz Ice Shelf, Marie Byrd Land, and partially along the western side of the AP (Fig. 3c). Seasonally, the direct effect of the longitude of the high pressure grows and expands during winter from both marine areas of the AP (Fig. 3i), with a stronger spatial correlation (up to 0.6) across the entire Weddell Sea and negative correlation over the Abbot Ice Shelf in spring (Fig. 3j). For the summer season, the positive feedback of precipitation remains along the eastern coastline of the AP, while a negative correlation occurs in some areas of the Amundsen Sea (Fig. 3k). The autumn area with a positive total precipitation relationship expands around the AP with values of about 0.4 to 0.5 (Fig. 3l).

The distance between the lowest and highest pressures has a direct average impact with correlation up to 0.5 over the southern part of the Amundsen Sea and near the Getz Ice Shelf on annual (Fig. 3b) and seasonal (Fig. 3m–p) precipitation totals, with the exception of the autumn, where

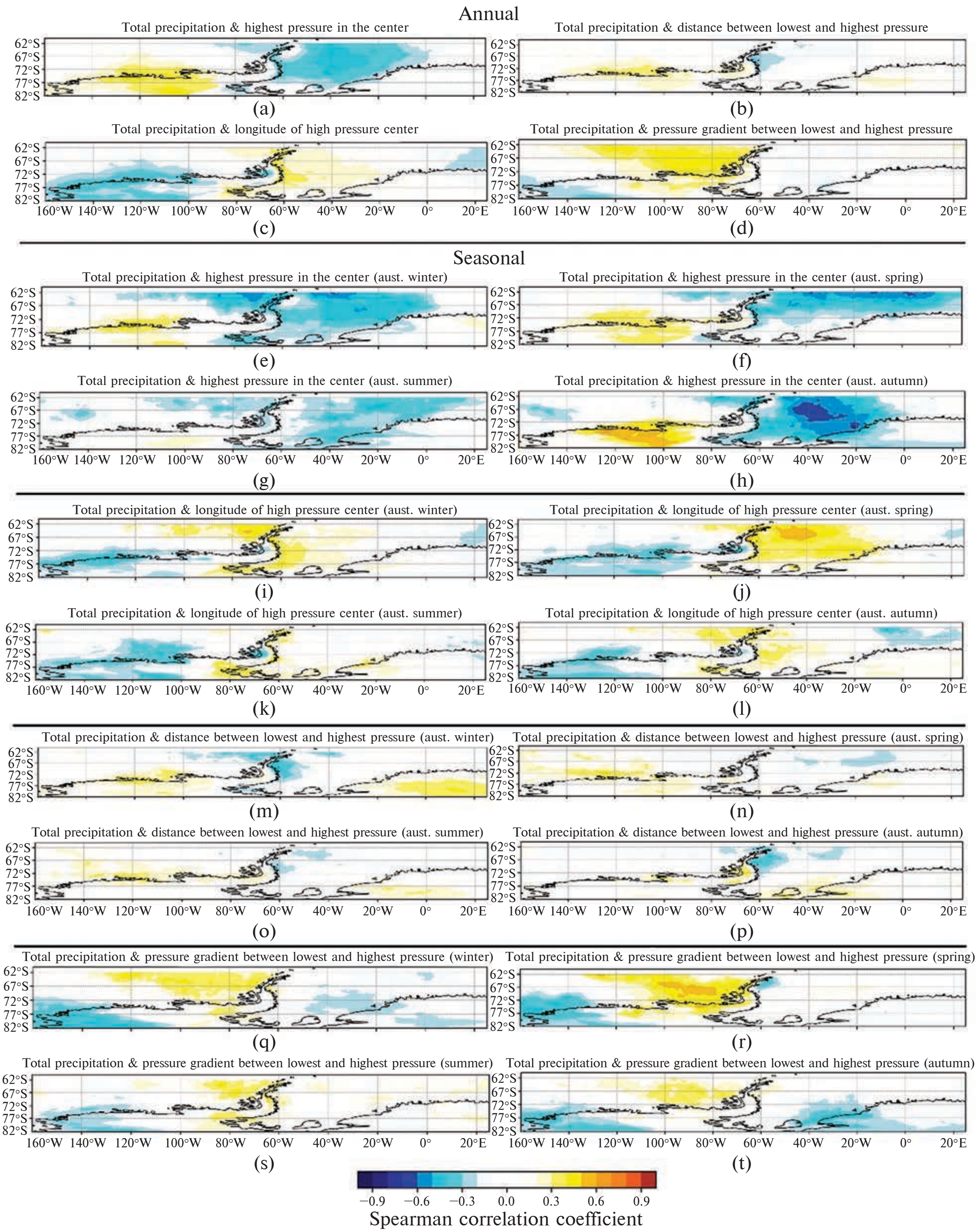

Figure 3. Spatial distribution of the Spearman correlation coefficient between precipitation totals and pressure parameters with the most significant dependences: the highest pressure in the center (a, e–h) and its longitude (c, i–l), distances between pressure centers (b, m–p), and spatial gradient between pressure centers (d, q–t)

such values are typical for the AP. Moreover, during the autumn and winter seasons, the opposite effect prevails over the eastern side of the AP with a correlation of −0.4 to −0.5. Overall, a larger distance results in greater precipitation on the western side of the studied polygon, where the domain is mainly under the influence of the ASL. Meanwhile, in areas adjacent to the AP, an opposite effect is observed during autumn and winter. In contrast to the distance between the lowest and the highest pressures, the gradient has demonstrated a significant effect on precipitation totals over the whole Bellingshausen Sea for annual values (Fig. 3d) and during spring (Fig. 3r) (correlation up to 0.6). A stronger pressure gradient is associated with higher precipitation totals (Fig. 3q–t). The inverse relationship is typical for the southwestern parts of the Amundsen Sea, near the Getz Ice Shelf and Marie Byrd Land, for the winter and spring (Fig. 3q, r).

In addition to total precipitation, it is necessary to evaluate the influence of pressure characteristics on the frequency of various phases.

The frequency of snow

The frequency of snow has a negative relationship with correlations up to −0.6 with the lowest pressure in the center (Fig. 4a, c–f), especially over the marine area of the Amundsen Sea, where the ASL climate pattern prevails. Additionally, this influence covers the neighbouring Thwaites Glacier, Pine Island glaciers, Abbot Ice Shelf, Ellsworth Land, and the AP with the strongest spatial correlation on an annual basis (Fig. 4a) and in spring (Fig. 4d). Notably, positive correlations of up to 0.7 were observed over Marie Byrd Land for yearly, spring (Fig. 4d), summer (Fig. 4e) and autumn (Fig. 4f) values. This indicates that a more intense low pressure is associated with a reduction in snowfalls. Moreover, during winter (Fig. 4c) and spring (Fig. 4d), moderate positive relationships (up to 0.6) were also observed over the Bellingshausen Sea, adjacent to the northwestern side of the AP (the Weddell Sea), and near the northeastern part during spring and summer.

The highest pressure exerts a moderate influence, being positively correlated (up to 0.4) with the frequency of snow in Marie Byrd Land, Getz Ice Shelf, Thwaites Glacier, and Dronning Maud Land but negatively correlated in the southern Weddell Sea annually (Fig. 4b). During winter (Fig. 4g) and autumn (Fig. 4j) such inverse correlations strengthen and expand in the aforementioned area of the Weddell Sea. Meanwhile, in autumn (Fig. 4j), positive correlations are also observed along the marine coastline of the Getz Ice Shelf, Thwaites Ice Shelf, and the northern and eastern parts of the Weddell Sea. During winter (Fig. 4g) and summer (Fig. 4i), the highest pressure has the opposite effect on the frequency of snow with correlations up to −0.5 in the Amundsen Sea and in the northern, western, and southern areas of the AP and also up to −0.4 in the Bellingshausen and Weddel Seas in spring (Fig. 4h).

The longitude of low pressure has a regional and uneven impact on the frequency of snow (Fig. 4k, l). On an annual and autumn scales, the frequency of snow days correlates negatively over the coast of the Getz Ice Shelf, Marie Byrd Land, and marine areas adjacent to the AP (localised areas of the Bellingshausen and the Weddell Seas). Throughout the year and in almost all seasons, positive relationships (up to 0.6) are observed in the northern and southern parts of the AP and over the Abbot Ice Shelf. The most contrasting season is winter (Fig. 4k): the eastward shift of the low-pressure center caused a decrease in the frequency of snow over the Getz Ice Shelf and an increase over the main areas of the Amundsen Sea, the Abbot Ice Shelf, and the south of the AP, with some adjacent regions of the Weddell Sea.

The annual relationship of the frequency of snow with the longitudinal position of the high-pressure center shows a similar spatial pattern of correlations with the longitude of the low-pressure center across the continent, but with lower values. They are around −0.4 over the Getz Ice Shelf and 0.4 over the Abbot Ice Shelf, southern parts of the AP, and adjacent areas of the Weddell Sea. There are positive links with the longitude of the high pressure during winter and spring over

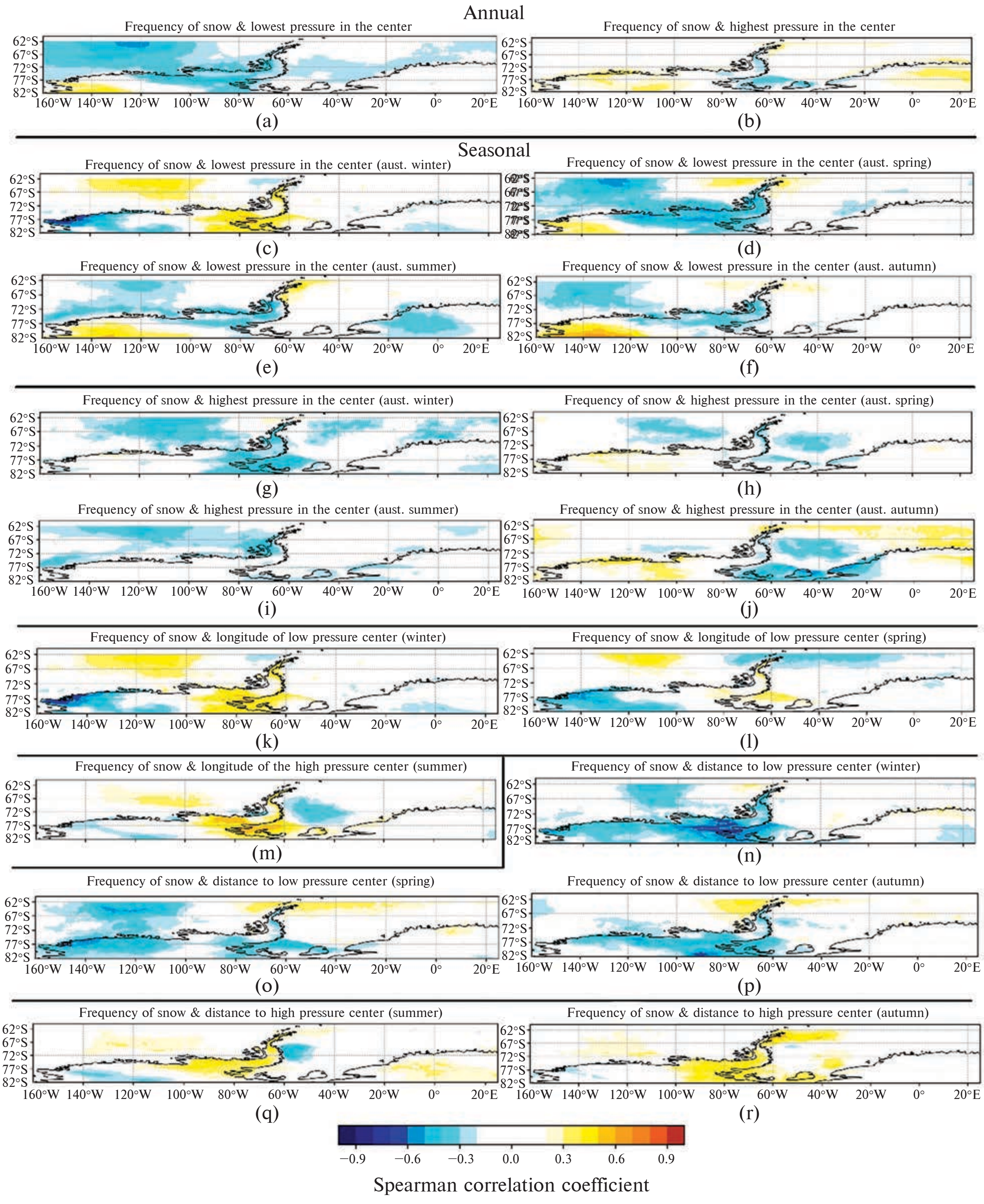

Figure 4. Spatial distribution of the Spearman coefficient for the correlation between frequency of snow and the pressure parameters with the most significant dependences: the lowest (a, c−f) and the highest (b, g−j) pressures in the centers, their longitudes (k−m), and distances (n−r)

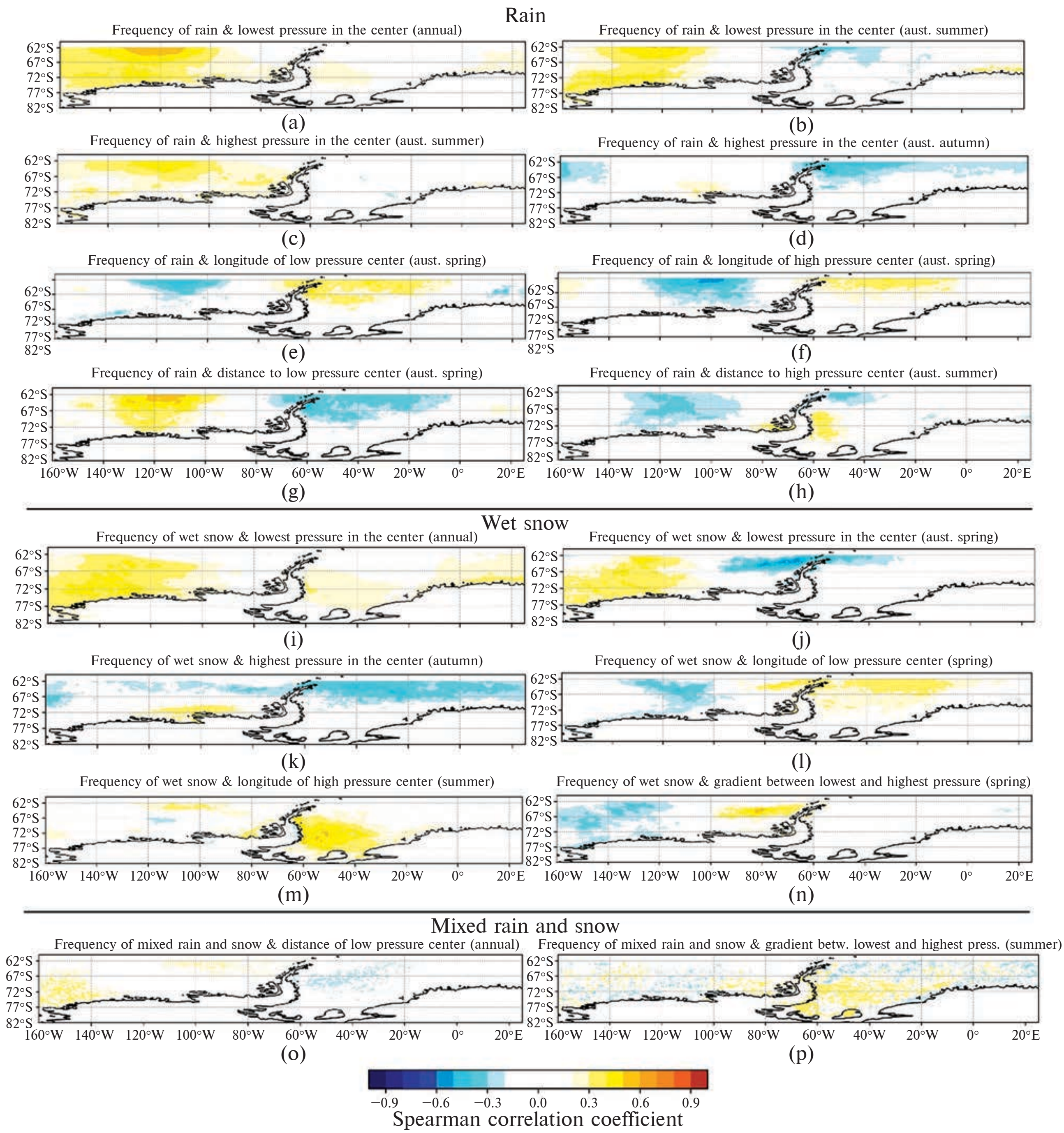

Figure 5. Spatial distribution of the Spearman correlation coefficient with the most significant dependences between pressure parameters and frequency of rain (a—h), wet snow (i—n), and mixed rain and snow (o, p)

the Amundsen Sea, with the most profound impact on snow in the summer (Fig. 4m). The bigger part of the AP, the Abbot Ice Shelf, and adjacent marine territories of the Weddell Sea are affected by positive correlations. Thus, an increase in the longitudinal position (i.e., eastward shift) of the

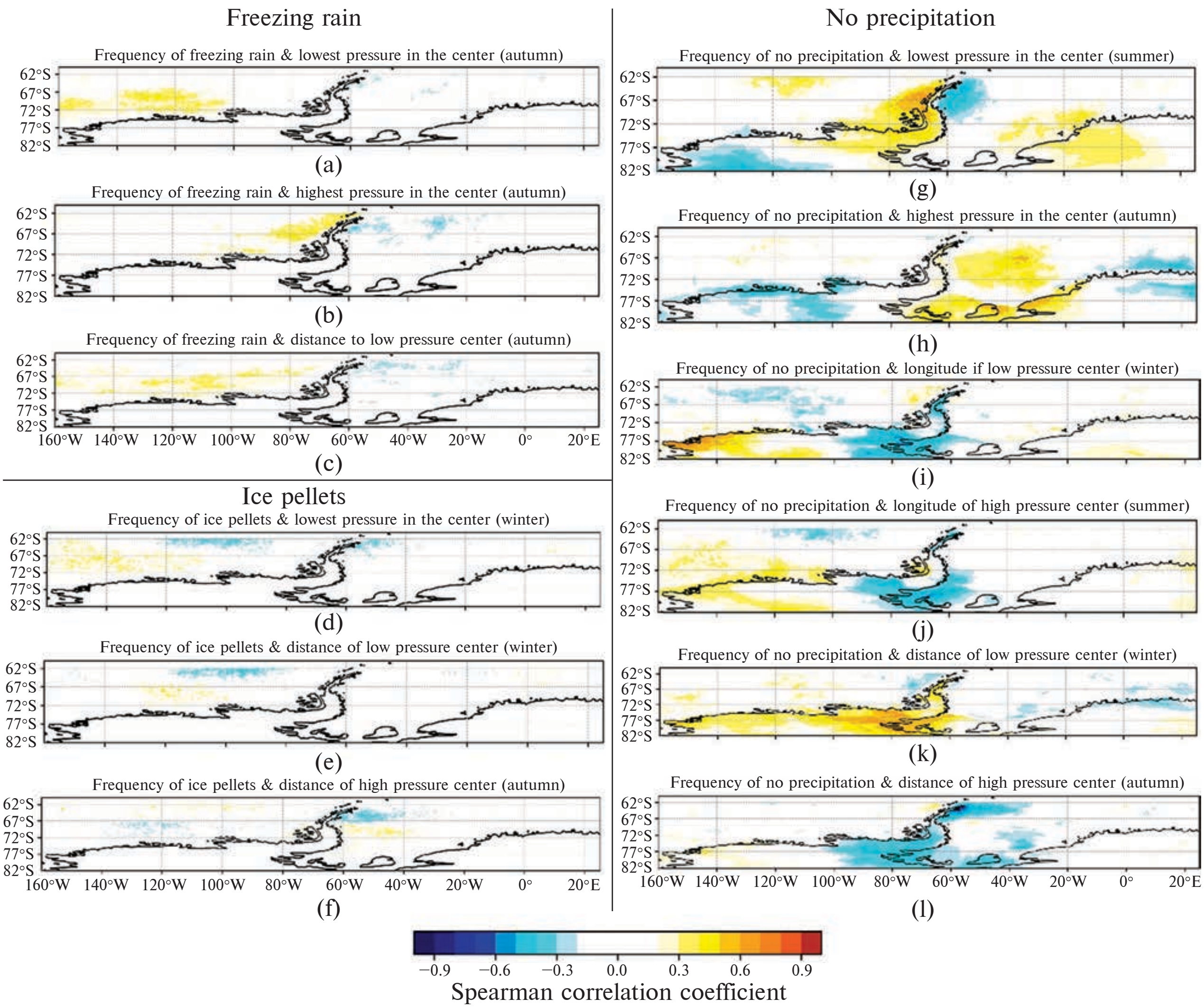

Figure 6. Spatial distribution of the Spearman correlation coefficient with the most significant dependences between pressure parameters and frequency of freezing rain (a–c), ice pellets (d–f), and the period with no precipitation (g–l)

high-pressure center can lead to more snow days; meanwhile, in some areas of the Weddell Sea, it could have the opposite effect during the summer.

Overall, the frequency of snow is negatively correlated (up to −0.6) with the distance to the low-pressure center over Thwaites Glacier, the Abbot Ice Shelf, part of the Filchner-Ronne Ice Shelf, northern and eastern AP, and the southern part of the Weddell Sea, both annually and across all seasons (Fig. 4n).

In addition, during the winter (Fig. 4n) and spring (Fig. 4o), a zone of moderate negative correlations forms over the Amundsen Sea, where the ASL is located, and in adjacent areas such as the Getz Ice Shelf. This implies that the shorter distance to the low-pressure center contributes to the growing frequency of snow. However, the opposite effect is observed in the marine areas of the Amundsen and Weddell Seas. These values of up to 0.5 are typical for the entire year, spring (Fig. 4o), and autumn (Fig. 4p). Therefore, a shorter distance could cause a decrease in snow. These regions could be affected by orographical conditions.

In contrast to the distance to the low-pressure center, the distance to the high-pressure center is likely to have the opposite effect concerning the AP and nearby territories. Correlations are generally moderate to moderately high (0.4—0.6), with the strongest impact on snow frequency during summer and autumn (Fig. 4q—r). A larger distance is associated with an increased frequency of snow events. Notably, a negative correlation zone (down to −0.5) emerges in summer along the eastern coast of the AP (Fig. 4q), whereas positive correlations persist east—northeast of the AP in winter, spring, and autumn, peaking in autumn (Fig. 4r). These spatial patterns partly mirror those linked to the distance from the low-pressure center in spring and autumn. However, over the Amundsen Sea, the relationship with the high-pressure center remains positive during winter and spring, in contrast to the low-pressure signal.

The distance between the lowest and highest pressures has an inverse effect on the snow frequency only along the eastern marine coast of the AP during winter, with values up to −0.4. There is no significant influence either annually or seasonally. The pressure gradient directly affects the frequency of snow over the Thwaites Ice Shelf, Pine Island Glaciers, and Abbot Ice Shelf, with positive correlations for all seasons. Snow days are more strongly positively influenced by pressure gradients spatially during winter and spring, including the northern part of the AP. However, during these seasons, there are also negative relationships up to −0.5 in the Bellingshausen Sea, and the same values over Marie Byrd Land, but only in winter. Positive correlations are found for the area of the Amundsen Sea on an annual basis and for spring and summer. It means that an increase in the pressure gradient predominantly causes a rise in the frequency of snow, although in some areas it may have the opposite effect.

The frequency of rain

The frequency of rain shows a moderate to moderately strong association (0.4 to 0.6) with the ASL central pressure over the Amundsen Sea across all seasons (Fig. 5a, b). However, there is a negative correlation near the northern part of the AP during the winter season. That implies that an increase in low pressure could lead to more frequent rain. The highest pressure positively influences the rain occurrence mostly during winter and summer over the Amundsen Sea (Fig. 5c), with an opposite dependence in autumn over the northern part of the Weddell Sea (Fig. 5d).

The longitude of the low-pressure center has a direct, moderate influence on the rain occurrence with an annual correlation of 0.4 over most of the Weddell Sea and adjacent areas of the Bellingshausen Sea near the AP. A similar pattern, but with smaller spatial coverage, was observed during the transitional seasons of spring and autumn (Fig. 5e). This suggests that an eastward shift of ASL can cause an increase in frequency of rain for the aforementioned regions throughout the year, in spring and in autumn. In winter, spring, and summer, the longitudinal position of low pressure over the Amundsen Sea leads to the opposite effect, with average negative correlations up to −0.5.

The frequency of rain is negatively correlated with the longitudinal position of high pressure across all seasons, resembling the relationship observed with the longitude of the low-pressure center. The strongest influence is also evident in the spring season, with the occurrence of rain responding positively to the longitude of the high-pressure center (Fig. 5f). These dependences partially coincide with the spatial correlations associated with the longitudinal position of the low-pressure center.

Regarding the distance to the low-pressure center, it generally has an inverse effect on rainfall compared to its longitudinal position. The marine parts of the Bellingshausen and Weddell Seas near the AP show negative correlations up to −0.4 annually, during spring (see Fig. 5g) and autumn, and positive correlations in the Amundsen Sea during winter and summer. The frequency of rain had a negative relationship with the distance to the high-pressure center in some areas of the Amundsen and Weddell Seas across all seasons, but with varying spatial coverage. Additionally, in summer, there is a positive relationship near the eastern part of the AP (Fig. 5h).

The distance between the lowest and highest pressures has demonstrated no significant effect on the rain occurrence, except in some localised marine areas of the Bellingshausen Sea during summer. The pressure gradient had a moderate negative correlation of −0.4 over some localised areas of the Amundsen Sea across all seasons, except winter. Also, the frequency of rain positively correlates with pressure gradient in the Bellingshausen Sea during spring and in the northern part of the Weddell Sea in summer.

The frequency of wet snow

Across all seasons, the lowest pressure in the center has average positive impact on the frequency of wet snow over the marine region of the Amundsen Sea, governed by the ASL climate pattern (Fig. 5i, j). The lower the central pressure, the more frequent wet snow is. Meanwhile, during winter and spring, negative correlations (up to −0.5) were detected over the northeastern regions of the Bellingshausen Sea (Fig. 5j). Similarly to the lowest pressure, the highest pressure impacts positively on the frequency of wet snow, being localised in specific areas over Amundsen Sea (at seasonal basis, not annual). In the northern part of the Weddell Sea, an inverse correlation of up to −0.5 was observed (Fig. 5k); there, an increase in pressure can lead to a decrease in the frequency of wet snow (apart from the summer season).

A higher longitude of the low-pressure center (eastward shift) has a positive effect on the frequency of wet snow over a broad area of the Weddell Sea, with an average correlation of 0.4 annually. The same pattern, but to a lesser extent, is common for spring, summer, and autumn (Fig. 5l). During spring and autumn, the longitudinal position of low pressure also influences the eastern part of the Bellingshausen Sea near the west coast of the AP. During winter and spring, the number of days with wet snow shows an average negative correlation across some locations in the Amundsen Sea. Thus, an increase in the longitude of the low pressure could lead to a decrease in wet snow occurrence in the Amundsen Sea. The longitude of high pressure also shows a direct impact on the frequency of wet snow (similar to the longitude of low pressure in spring); however, the more profound impact is in summer with correlations up to 0.6 in the Weddell Sea and near the eastern marine coast of the AP (Fig. 5m). Similarly to the low pressure, the longitude of the high pressure has also negative average relationships in the area of the Amundsen Sea.

The distance to low pressure had a moderate negative impact (up to −0.5) on the frequency of wet snow over the eastern Bellingshausen Sea and the northern Weddell Sea, both annually and in winter and spring. Meanwhile, for the Amundsen Sea, reverse correlations were obtained. The annual distance to the high pressure has a local negative influence on the frequency of wet snow over the Amundsen and Weddell Seas. However, this impact was observed in the northern part of the Amundsen Sea and near the AP during summer and autumn.

The frequency of wet snow weakly correlates with the gradient between the lowest and highest pressures. On an annual basis, the gradient between the lowest and highest pressures produces the opposite effect on the frequency of wet snow in parts of the Amundsen and Weddell Seas, with correlations up to −0.5. Such impact persists in some localised areas in spring and summer (Fig. 5n), whereas in winter and spring in the Bellingshausen Sea, there is a moderate positive relationship.

The frequency of mixed rain and snow

Overall, the frequency of mixed rain and snow weakly correlates with the lowest pressure and its longitude across seasons, except in some localised areas on an annual basis. Regarding the highest pressure, some areas of the Amundsen, Bellingshausen, and Weddell Seas exhibit both moderate positive and negative correlations in spring and autumn. The longitude of the highest pressure does not influence the frequency of mixed rain and snow.

Distances to the low-pressure center and between the lowest and the highest pressures demonstrate a positive impact on the frequency of mixed snow and rain in certain areas of the western Amundsen Sea, both annually and during winter, with correlations of 0.4 (Fig. 5o). Meanwhile, the distance to the highest pressure center shows no influence. The pressure gradient between the lowest and highest pressures has a positive impact on the frequency of mixed snow and rain in the southern Bellingshausen Sea and over areas of the Weddell Sea and near the eastern coastline of the AP (Fig. 5p).

The frequency of freezing rain

The lowest pressure in the center influences the frequency of freezing rain mainly in the marine area of the Amundsen Sea either on an annual or seasonal basis (Fig. 6a). Overall, the freezing rain correlates with the highest pressure with the most significant relationship (up to 0.5) in the eastern part of the Bellingshausen Sea (Fig. 6b). Thus, lower central pressure may result in a reduced frequency of freezing rain in the Amundsen Sea during certain seasons, whereas higher pressure – in the increased frequency in the eastern part of the Bellingshausen Sea near the western coast of the AP for transition seasons.

The frequency of freezing rain is moderately positively correlated with both the longitude and the distance to the low-pressure center in spring, but in different regions: correlations of 0.4 over the Weddell Sea for the longitude and 0.5 over the Amundsen Sea for the distance to the ASL center. There is also a moderate link for the autumn for the latter characteristic (Fig. 6c). It should be noted that the distance to high pressure does not have any significant impact on the frequency of freezing rain. The same is relevant for the distances to the high-pressure center and between the lowest and the highest pressures, as well as for their pressure gradient (except for localised areas in the Amundsen Sea in spring).

The frequency of ice pellets

The lowest pressure center exerts a moderate influence on the frequency of ice pellets in the northern parts of the Amundsen and Bellingshausen Seas, demonstrating a negative relationship of −0.4 for both annual and seasonal values (Fig. 6d), except in summer. Therefore, a deepening of the low pressure in the center may induce an increase in the frequency of ice pellets over the northern areas of the aforementioned seas. Additionally, in winter, some areas with positive correlations are seen in the central part of the Amundsen Sea. There is a similar pattern for the highest pressure in the center, but for winter and summer.

The longitudinal positions of the low- and high-pressure centers have an average influence on ice pellets only in winter, but with the reverse correlation of −0.4 (Fig. 6e) in the same region, in contrast to the effect of the central lowest pressure. Also, during spring, there are scattered spots with positive correlations in the Weddell Sea. The distance to low pressure has an effect on the frequency of ice pellets similar to that of the lowest pressure in the center; however, it holds only for winter. Meanwhile, the distance to high pressure in winter shows a positive correlation (around 0.4) in the northern part of the Amundsen Sea that has a pattern similar to the longitudinal position of the high pressure. For autumn, there are neighbouring areas in the Weddell Sea with contrasting influence: −0.4 in the northern sector near the AP and 0.4 in the more southern sector (Fig. 6f). The frequency of ice pellets shows either no correlation or only weak correlations with the pressure gradient between the lowest- and highest-pressure centers, as well as with their distance.

Frequency of periods with no precipitation

The most pronounced and contrasting effect of the lowest pressure on precipitation-free periods is observed in summer (Fig. 6g). Notably, a deepening pressure may contribute to the shortening of the no-precipitation period with moderate-high correlations up to 0.7 in areas adjacent to the Bellingshausen Sea near the west coast of the AP and to the north of it. Meanwhile, near the northeastern coast of the AP, the influence is opposite. Thus, a pressure decrease causes a reduction in the frequency of no-precipitation periods. It can also be related to the AP orography. The highest pressure in the center exerts a direct impact on the precipitation-free period more in autumn and over the Weddell Sea (Fig. 6h). The longitudinal positions of the low- and high-pressure centers both affect the no-precipitation period in opposite ways, but during different seasons: the low-pressure center in winter and the high-pressure center in summer with correlation up to −0.5 (Fig. 6i, j). Thus, the higher longitudes of these pressures cause a decline in the no-precipitation period, but for different seasons. Distance to the low-pressure center during winter has a positive impact with correlations up to 0.6 on the frequency of periods with no precipitation in the southern part of the AP and the Abbot Ice Shelf and the southern Weddell Sea (Fig. 6k). The longer the distance, the longer the precipitation-free period. The distance to high pressure has an opposite influence on this meteorological characteristic over all the AP and the adjacent northeastern marine areas of the Weddell Sea during autumn (Fig. 6l). Consequently, a shorter distance to the high-pressure center results in a higher frequency of the no-precipitation period.

3.3.2 Impact of pressure parameters on near-surface air temperature and dew point

The correlations between pressure parameters and near-surface air temperature and the dew point were generally weak to moderate and varied across seasons. Overall, annual near-surface temperature has shown a small direct association with the lowest pressure in the center (Fig. A2a). However, moderate correlations are found in specific areas of the ASL, as well as in the eastern part of the Bellingshausen Sea close to the AP. Thus, in some separate areas, the deepening of the low pressure can lead to a slight increase in air temperature on an annual basis (Fig. A2a). Meanwhile, there is no significant link between seasonal values. At the same time, the highest pressure has an opposite effect in the Weddell Sea and adjacent continental territories of Dronning Maud Land, including an area to the south from the AP (Fig. A2b). For the transition seasons (spring and autumn), moderate negative correlations are also observed in different locations. For the autumn, most correlations are associated with the northern parts of the Amundsen and Bellingshausen Seas, Abbot Ice Shelf, and Pine Island Glaciers (Fig. A2c). Thus, in high latitudes, higher pressures correspond to lower temperatures.

The annual longitude of low pressure exerts both weak and moderate impacts on the 2-m air temperature. The most profound effect with a value of 0.4 is for the western part of the Amundsen Sea, Getz Ice Shelf, Mary Byrd Land, and the marine coast of the Weddell Sea (Fig. A2d). The seasons showed either no connection or a very weak one. The exception occurred in summer, when the longitude of the high pressure positively affects the near-surface temperature of Dronning Mode Land, especially along the marine coast (Fig. A2e).

The annual distance to the low-pressure center has a positive dependence on the 2-m air temperature, with a value of about 0.4 only in the western part of the Amundsen Sea, the adjacent Getz Ice Shelf, and Marie Byrd Land (Fig. A2f). For the summer, such positive relationships are defined for marine areas to the northeast of the AP and in the Amundsen Sea (Fig. A2g). This implies that a greater distance to the low-pressure center induces the annual temperature increase and *vice versa*. Meanwhile, a bigger distance to the high pressure might contribute to decreasing air temperature for the eastern part of the Weddell Sea with coastline in winter and summer (Fig. A2h, i).

The spatial distribution of correlations for the dew point often shows patterns similar to those for the air temperature; however, some dependencies are more or less pronounced. Overall, the lowest central pressure itself makes a weak positive impact on the dew point annually. Moderate correlations were observed only in some spots of the ASL location and near the western part of the AP (Fig. A2j). The same is also relevant for the winter season. Compared with its association with the minimum pressure, the highest pressure exerts a more significant spatial influence, exhibiting a moderate negative correlation both annually and during the spring and autumn transitions (Fig. A2k). It covers rather big areas, especially on the annual scale, including the Weddell Sea and adjacent continent territories to the south of the AP and Dronning Maud Land. A stronger air pressure leads to stronger downward air movements and a lower dew point. During the transitional seasons, such spatial relationships are more heterogeneous, as shown for autumn.

Overall, the annual 2-m dew point demonstrated positive weak and moderate correlations (with values up to 0.4) with the longitudinal position of the low-pressure center that, for this particular region, is associated with the climate pattern of ASL, including the nearby Getz Ice Shelf and Mary Bird Island (Fig. A2l). It means that shifting the ASL center towards the east causes the growth of 2-m dew points (for the annual scale). The longitude of high pressure has shown a positive mean impact on the 2-m dew point only in summer along the marine coast of the Weddell Sea and in Dronning Maud Land (Fig. A2m).

The distance to the low-pressure center moderately affects the 2-m dew point with positive correlation in the field of ASL location (Fig. A2n). During the summer, the distance to the low pressure (Fig. A2o) demonstrated the opposite effect in the northeastern marine area near the AP compared to the center's longitude. For the distance to high pressure, negative relationships have been detected only in the eastern localised marine area of the Weddell Sea during winter and along its coastline during summer (Fig. A2p). The latter outcome is the opposite of the obtained positive links found with the longitude of high pressure (see Fig. A2m) and at the same time resembles the spatial pattern for the 2-m air temperature.

The distance between the lowest and highest pressures demonstrated opposite effects and different spatial impacts on the 2-m dew point during the spring and summer seasons. For spring, we detected correlations up to −0.4 for the southern marine areas of the Amundsen Sea, the adjacent Getz Ice Shelf, Marie Bird Land, the southern waters of the Weddell Sea, and the area to the south of the AP (Fig. A2q, r). In contrast, the 2-m dew point in summer has a positive link with the maritime area of the Weddell Sea, east of the AP. This suggests that the decrease in distance between the lowest and highest pressures resulted in the growth of the 2-m dew point in the above mentioned regions for spring. The inverse dependence was observed in the northwestern part of the Weddell Sea near the AP for summer.

The gradient between the lowest and the highest pressures (Fig. A2s) showed negative correlations (up to −0.4) with the 2-m dew point on an annual basis. It implies that the 2-m dew point variability depends on the highest pressure, especially over the Weddell Sea and adjacent territories such as AP and Dronning Maud Land. Moreover, the dependence of the 2-m dew point on the highest pressure determined its dependence on the pressure gradient. Throughout the summer season, the negative correlation persists in the Weddell Sea, reaching even stronger values of up to −0.5 in some areas.

3.3.3 Impact of pressure parameters on wind components

Similarly to the air temperature and dew point, there are moderate and weak correlation coefficients between pressure parameters and wind components. Generally, there are no significant relationships between the wind's *u*-component and the lowest and the highest pressures. However, localised positive moderate correlations up to 0.4 were found annually along the eastern coast and on the south of the AP (Fig. A3a, b). Also, changes in the *u*-component are not strongly associated with the longitudes of either low- or high-pressure centers (Fig. A3c), except for summer when negative correlations appeared to the south from the AP and on the eastern part of the Weddell Sea, Dronning Maud Land (Fig. A3d).

The distance to the low-pressure center affects the *u*-component of wind, with a positive connection on the marine coast of the Getz Ice Shelf and Mary Bird Island for annual values (Fig. A3e) and for the Dronning Maud Land in summer. The high-pressure center has an average positive impact on the *u*-component of the wind in the eastern coastline of the Weddell Sea during the winter season (Fig. A3f).

In the spring season, the greater the distance between the lowest and highest-pressure centers, the greater the increase in the *u*-component of the wind (western winds) in the localised areas of the Amundsen Sea and the southern part of the Weddell Sea, which is supported by correlations of up to 0.4 (Fig. A3g). In contrast to the relationship with the distance between the lowest- and highest-pressure centers, the *u*-component demonstrates a reverse moderate negative dependence on the pressure gradient along the narrow marine coast of the Weddell Sea, both in summer and on an annual basis.

The wind's 10-m *v*-component has no significant spatial link with the minimum central pressure, either annually or seasonally (for example, see Fig. A3h). Contrary to that, these relationships are found for the maximum central pressure (up to −0.4) in the western part of Marie Byrd Land annually and along the coast to the south from the AP annually and in spring) (Fig. A3i). This fits with the intensification of the high-pressure center causing a decrease in the *v*-component (more northern winds) in the western regions and an increase (more southern winds) near the AP, respectively.

The wind's *v*-component generally shows no or a very weak correlation with the longitudinal position of the minimum pressure center (Fig. A3j), except for the transitional seasons having negative dependences in the sectors to the south of the AP and in the western part of the Amundsen Sea (Fig. A3k).

The distance to the low pressure causes moderate changes (approximately with correlation up to 0.4) in the wind's *v*-component over the western parts of the Getz Ice Shelf and Marie Byrd Land on an annual basis (Fig. A3l). This is expected, as this region is influenced by the ASL climate pattern. Additionally, during the winter season, a localised area with negative values appears in the Weddell Sea near the eastern coastline of the AP. The *v*-component showed a localised positive correlation with distance to the high-pressure center in winter, particularly near the western side of the AP.

Links between the *v*-component and the distance between areas of the lowest and highest pressures are generally weak, with the exception of the south-eastern part of the AP (Fig. A3m). In contrast, the pressure gradient has a greater impact on the near-surface *v*-component in some areas for annual characteristics. Overall, annual dependency has rather mosaic moderate correlations (Fig. A3n). Relationships are negative in the west of the Getz Ice Shelf and Marie Byrd Land in some locations, indicating that a larger pressure gradient leads to a decrease in the wind's *v*-component (less southern winds). In contrast, positive relationships are observed along the southern marine coastal sector of the AP. In this case, a stronger pressure gradient results in a growing *v*-component in these specific zones. To the east of the AP, near the coastline, both negative and positive moderate annual correlations are found. However, seasons showed weak statistical relationships.

4 Discussion

This study was conducted to estimate relationships between pressure parameters and meteorological characteristics, which may improve the quality of weather forecasting and enhance the understanding of atmospheric processes, particularly in the Antarctic region, which remains insufficiently explored due to the scarcity of meteorological observations.

As shown in our analysis, the climatic pressure dipole consisting of the ASL and the high-pressure area in the western Weddell Sea plays a significant role in weather variability over the AP and adjacent marine regions. Their interaction is particularly important in West Antarctica and the AP, where thermodynamic processes are the main contributors (Turner et al., 2025; Wang et al., 2025). It has been suggested that the ASL itself results from the interaction between Antarctic topography and the westerly wind jet (Goyal et al., 2021), and that it is deepening (Raphael et al., 2016). Our analysis confirmed this, showing that ASL deepening is the only statistically significant trend among a range of pressure parameters.

Wang et al. (2021) demonstrated that a deeper ASL is associated with increased rainfall in the Amundsen and Bellingshausen Seas. However, our results suggest a more complex pattern, which we attribute to two additional features beyond ASL depth: its geographical location and the distance of a region from the low-pressure center. Specifically, closer to the ASL, snowfall can increase over marine areas, whereas nearer the AP, precipitation tends to shift to mixed or liquid phases, and overall precipitation becomes more frequent. This indicates that the influence of the ASL on meteorological conditions is not spatially homogeneous and varies by season (Raphael et al., 2019). Moreover, regional pressure patterns that strongly impact weather are themselves driven by larger-scale processes (Lim et al., 2016; Orr et al., 2023).

Considering these results, the possible biases in the representation of precipitation types in ERA5 should be taken into account. While the general distribution and dependencies are unlikely to be strongly affected, certain features and quantitative estimates may be biased. These biases may be related both to precipitation parameterisations and to the representation of temperature conditions (Vignon et al., 2021). The latter is particularly important for the indirectly estimated precipitation types such as wet snow, freezing rain, snow pellets, and mixed precipitation. In particular, biases in determining the melting layer and in estimating liquid water content may be among the main reasons for the occurrence of biases in the quantification of precipitation types (ECMWF, 2025b). Overall, the longitudinal position of the ASL affects the spatial distribution of thermal regimes across West Antarctica and the AP (Clem et al., 2017). Previous research (Pysarenko et al., 2023) identified several key dependencies: a westward ASL shift decreases precipitation over the Amundsen Sea and increases it over the AP; ASL deepening reduces precipitation over the Getz Ice Shelf but enhances it over the western AP. The results presented here expand on those findings, revealing additional dependencies crucial for weather formation over the Amundsen and Bellingshausen Seas, including the coastal areas of West Antarctica.

The AP acts as a barrier that modifies precipitation formation depending on its windward and leeward sides (Turner et al., 1998). Differences in snowfall formation have been linked to frontal depressions and to northern flow under blocking conditions. We also identified a chain-like interaction between the ASL and regional meteorology: the ASL affects winds northwest of the AP, which in turn modulate foehn winds and advection, leading to air temperature changes, including those responsible for warming (Zhang et al., 2021). Depending on pressure configurations, however, cooling effects may also arise from other wind directions.

The spatial configuration of the climatic dipole further contributes to extreme events. For instance, pressure patterns favourable for the formation of Antarctic atmospheric rivers often trigger large precipitation events (Wille et al., 2021). Warm-air intrusions increase the frequency of rainfall days over the western AP, whereas in the eastern AP, rainfall is less frequent (Vignon et al., 2021). Westerly winds in the region can develop into two distinct regimes — “blocked” and “flow-over” — both of which act as warming mechanisms (Orr et al., 2008). Conversely, anomalous southerly winds advect colder and drier air into the Bellingshausen–Weddell Seas and the AP, reducing precipitation (Chen et al., 2023). These pressure-driven processes also affect sea ice: for example, a negative correlation has been reported between moisture sinks and sea-ice concentration (Reboita et al., 2019). This implies that the observed changes in precipitation amount and phase may cause significant variability in sea ice across the region.

Among the factors influencing precipitation, orography is particularly important. For example, steep terrain can intensify the rainfall events due to the interaction of atmospheric rivers with complex orography (Gilbert et al., 2025). In contrast, higher temperatures are frequently associated with orographic influences via foehn warming with less precipitation (Turner et al., 2021). Orography appears to be crucial for the spatial distribution of freezing rain and ice pellets. Although these phases occur infrequently, our results show that they strongly depend on the orography of the AP. The formation of freezing rain in polar regions requires warm-air advection combined with orographic effects (Kochtubajda et al., 2017). Although that study was conducted in the Arctic, the northern AP exhibits similar conditions favourable for freezing rain. Ice pellets, by contrast, require refreezing processes (Tobin et al., 2023), which can also occur over the complex orography of the AP.

5 Conclusions

This study, based on the ERA5 reanalysis, focused on analysing the spatio-temporal patterns of meteorological variables and precipitation types in relation to the climatic pressure dipole (the ASL, with a climatological mean MSLP of 980 hPa, and the relatively high-pressure area over the Weddell Sea, with a mean MSLP of 990 hPa). Despite variability in the endpoints' locations, the dipole forms an average pressure gradient of 6.42 hPa per 1000 km, which defines the intensity of atmospheric zonal winds and meridional air penetration. No clear interannual tendencies were detected in the pressure parameters, except for a slight deepening of the ASL in recent decades.

The interaction between these relatively stable pressure patterns and the ocean–land distribution produces spatial variations in the thermal and wind regimes across the Amundsen–Bellingshausen–Weddell Seas domain. Consequently, precipitation types in the region are typically dominated by snow, with lower precipitation frequency in the interior of the continent and more frequent rainfall in the north. The presence of the AP further modulates precipitation distribution, contributing to an increased frequency of ice pellets and freezing rain, and a lower frequency of wet snow, particularly on its north-eastern side.

The ASL variability corresponded to changes in the frequency of snow, wet snow, and rain. Under a deeper ASL, the frequency of snowfall increases over the Amundsen and Bellingshausen Seas (while rainfall decreases), and precipitation shifts from snow to wet snow near the AP. A strong relationship was found between precipitation occurrence over the Weddell Sea and high pressure near the eastern part of the AP. The higher the pressure, the less precipitation is observed, especially during the transition seasons, with a significant decrease in snowfall and wet snow over the Weddell Sea and south of the AP, and a decrease in rain and freezing rain to the northeast of the AP.

Eastward shifts of the ASL, closer to the AP, led to increased snowfall over the Amundsen Sea and in the southern part of the AP, and to increases in rain and wet snow to the north and northeast of the AP. When the center of high pressure shifted eastward from the AP, precipitation over the Weddell Sea increased, mainly in the form of rain and freezing rain, with snow over marine areas often replaced by wet snow. In this situation, however, snowfall increased over the southern part of the AP. In general, more snow was observed in areas closer to the local pressure extrema: over the Amundsen Sea, closer to the ASL, and near the AP, closer to high pressure. Specifically, the closer the high-pressure center is located to the north of the AP during autumn, the more ice pellets occur in the region of their maximum frequency near the AP. Moreover, the closer the location and the stronger the pressure gradient in the region, the more snowfall occurred, especially over the Bellingshausen Sea.

In comparison to precipitation changes that respond strongly to the variability of the climatic pressure dipole, near-surface meteorological parameters exhibited less pronounced effects. In general, the deepening of the ASL tends to lower the air temperature and the saturation point over the eastern Bellingshausen Sea; however, ASL's eastward displacement mainly results in warmer conditions across the study region. A ridge of high pressure east of the AP can significantly influence the thermal regime over the Weddell Sea and Dronning Maud Land. In particular, colder conditions occur during periods of stronger pressure and its westward shift toward the AP. When the distance between the ASL and local high pressure over the Weddell Sea decreases, warmer conditions are observed across several regions, including the Getz Ice Shelf, Marie Byrd Land, the southern Weddell Sea, and areas south of the AP.

The most stable relationships for wind parameters were detected with the high pressure over the western Weddell Sea and with atmospheric circulation around the AP. Higher pressure was associated with the intensification of southerly and westerly winds in the southern part of the AP. The dependencies with the ASL were mostly related to the distance from the pressure center, with greater distances resulting in stronger westerly and southerly winds along the marine coast of the Getz Ice Shelf and Marie Byrd Land. However, additional smaller-scale dependencies were also identified, typically characteristic of certain seasons.

The obtained results can contribute to a better understanding of precipitation variability in the region. The present study, together with previously obtained results (Pysarenko et al., 2023), provides a detailed historical analysis that can serve as a basis for future investigations of precipitation changes, complementing existing analyses based on CMIP6 projections (Bracegirdle et al., 2020). As a significant factor influencing ecosystem formation in maritime Antarctica, precipitation variability in the region may also support studies of ice-shelf vulnerability in the Antarctic Peninsula (Višnjević et al., 2025).

Data availability. The data used for the study were derived from a publicly open dataset of the ECMWF ERA5 reanalysis (retrieved from https://cds.climate.copernicus.eu/datasets/reanalysis-era5-single-levels?tab=overview, accessed 15.08.2025).

Author contributions. Idea, conceptualization: D. P., L. P. Data preparation and processing: L. P., M. S. Research: L. P., D. P. Visualization: M. S., L. P. Initial draft: L. P., M. S. Writing: L. P., M. S., D. P. Reviewing, editing: D. P.

Funding. The study was funded within the framework of the project "Polar Regions in the Earth System" ("PolarRES"), which has received funding from the European Union's Horizon 2020 Research and Innovation Programme under Grant Agreement No. 101003590. This research was conducted within the framework of the State Special-Purpose Research Program in Antarctica for 2011–2025.

Conflict of Interest. The authors declare no conflict of interest.

References

Andres-Martin, M., Azorin-Molina, C., Serrano, E., González-Herrero, S., Guijarro, J. A., Bedoya-Valestt, S., Utrabo-Carazo, E., & Vicente Serrano, S. M. (2024). Near-surface wind speed trends and variability over the Antarctic Peninsula, 1979–2022. *Atmospheric Research*, *309*, 107568. https://doi.org/10.1016/j.atmosres.2024.107568

Ayres, H. C., Ferreira, D., Park, W., Kjellsson, J., & Ödalen, M. (2024). A comparison of the atmospheric response to the Weddell Sea Polynya in atmospheric general circulation models (AGCMs) of varying resolutions. *Weather and Climate Dynamics*, *5*(2), 805–820. https://doi.org/10.5194/wcd-5-805-2024

Ayres, H. C., Screen, J. A., Blockley, E. W., & Bracegirdle, T. J. (2022). The coupled atmosphere–ocean response to Antarctic Sea Ice Loss. *Journal of Climate*, *35*(14), 4665–4685. https://doi.org/10.1175/JCLI-D-21-0918.1

Boothroyd, A., Adams, V., Alexander, K., & Hill, N. (2024). Priority areas for marine protection in the Amundsen and Bellingshausen Seas, Antarctica. *Marine Policy*, *167*, 106232. https://doi.org/10.1016/j.marpol.2024.106232

Bracegirdle, T. J., Krinner, G., Tonelli, M., Haumann, F. A., Naughten, K. A., Rackow, T., Roach, L. A., & Wainer, I. (2020). Twenty first century changes in Antarctic and Southern Ocean surface climate in CMIP6. *Atmospheric Science Letters*, *21*(9), e984. https://doi.org/10.1002/asl.984

Cai, W., Gao, L., Luo, Y., Li, X., Zheng, X., Zhang, X., Cheng, X., Jia, F., Purich, A., Santoso, A., Du, Y., Holland, D. M., Shi, J.-R., Xiang, B., & Xie, S.-P. (2023). Southern Ocean warming and its climatic impacts. *Science Bulletin*, *68*(9), 946–960. https://doi.org/10.1016/j.scib.2023.03.049

Carrasco, J. F., Bozkurt, D., & Cordero, R. R. (2021). A review of the observed air temperature in the Antarctic Peninsula. Did the warming trend come back after the early 21st hiatus? *Polar Science*, *28*, 100653. https://doi.org/10.1016/j.polar.2021.100653

Chen, X., Li, S., & Zhang, C. (2023). Distinct impacts of two kinds of El Niño on precipitation over the Antarctic Peninsula and West Antarctica in austral spring. *Atmospheric and Oceanic Science Letters*, *16*(5), 100387. https://doi.org/10.1016/j.aosl.2023.100387

Clem, K. R., Renwick, J. A., & McGregor, J. (2017). Large-scale forcing of the Amundsen Sea Low and its influence on sea ice and West Antarctic temperature. *Journal of Climate*, *30*(20), 8405–8424. https://doi.org/10.1175/JCLI-D-16-0891.1

Dalaiden, Q., Abram, N. J., Goosse, H., Holland, P. R., O'Connor, G. K., & Topál, D. (2024). Multi-decadal variability of Amundsen Sea Low controlled by natural tropical and anthropogenic drivers. *Geophysical Research Letters*, *51*(16), e2024GL109137. https://doi.org/10.1029/2024GL109137

ECMWF. (2025a). *ERA5: Data documentation*. Retrieved October 20, 2025, from https://confluence.ecmwf.int/display/CKB/ERA5%3A+data+documentation

ECMWF. (2025b). Section 2.1.5.5 Types of Precipitation. In *Forecast User Guide*. Retrieved October 20, 2025, from https://confluence.ecmwf.int/display/FUG/Section+2.1.5.5+Types+of+Precipitation, https://doi.org/10.21957/m1cs7h

Gao, M., Kim, S.-J., Yang, J., Liu, J., Jiang, T., Su, B., Wang, Y., & Huang, J. (2021). Historical fidelity and future change of Amundsen Sea Low under 1.5 °C–4 °C global warming in CMIP6. *Atmospheric Research*, *255*, 105533. https://doi.org/10.1016/j.atmosres.2021.105533

Gilbert, E., Pishniak, D., Torres, J. A., Orr, A., Maclennan, M., Wever, N., & Verro, K. (2025). Extreme precipitation associated with atmospheric rivers over West Antarctic ice shelves: insights from kilometre-scale regional climate modelling. *The Cryosphere*, *19*(2), 597–618. https://doi.org/10.5194/tc-19-597-2025

Goyal, R., Jucker, M., Sen Gupta, A., & England, M. H. (2021). Generation of the Amundsen Sea Low by Antarctic orography. *Geophysical Research Letters*, *48*(4), e2020GL091487. https://doi.org/10.1029/2020GL091487

Hellmuth, F., Carlsen, T., Daloz, A. S., David, R. O., Che, H., & Storelvmo, T. (2025). Evaluation of biases in mid-to-high-latitude surface snowfall and cloud phase in ERA5 and CMIP6 using satellite observations. *Atmospheric Chemistry and Physics*, *25*(2), 1353–1383. https://doi.org/10.5194/acp-25-1353-2025

Hepworth, E., Messori, G., & Vichi, M. (2024). Synoptic-scale extreme variability of winter Antarctic sea-ice concentration and its link to Southern Ocean extratropical cyclones. *Journal of Geophysical Research: Oceans, 129*(6), e2023JC019825. https://doi.org/10.1029/2023JC019825

Hersbach, H., Bell, B., Berrisford, P., Biavati, G., Horányi, A., Muñoz Sabater, J., Nicolas, J., Peubey, C., Radu, R., Rozum, I., Schepers, D., Simmons, A., Soci, C., Dee, D., & Thépaut, J-N. (2023). ERA5 hourly data on single levels from 1940 to present. *Copernicus Climate Change Service (C3S) Climate Data Store (CDS)*. Retrieved August 15, 2025, from https://cds.climate.copernicus.eu/datasets/reanalysis-era5-single-levels?tab=overview, https://doi.org/10.24381/cds.adbb2d47

Hughes, K. A., Convey, P., & Turner, J. (2021). Developing resilience to climate change impacts in Antarctica: An evaluation of Antarctic Treaty System protected area policy. *Environmental Science & Policy*, *124*, 12–22. https://doi.org/10.1016/j.envsci.2021.05.023

Intergovernmental Panel on Climate Change (IPCC). (2022). *The Ocean and Cryosphere in a Changing Climate*. Cambridge University Press. https://doi.org/10.1017/9781009157964

Kochtubajda, B., Mooney, C., & Stewart, R. (2017). Characteristics, atmospheric drivers and occurrence patterns of freezing precipitation and ice pellets over the Prairie Provinces and Arctic Territories of Canada: 1964–2005. *Atmospheric Research*, *191*, 115–127. https://doi.org/10.1016/j.atmosres.2017.03.005

Li, R., Li, G., Hai, G., Xie, H., Cheng, Y., Chen, W., Cui, X., Ding, M., Gao, C., Hao, T., Ke, C., Li, C., Li, J., Liu, Y., Ran, J., Ren, J., Shen, Q., Shen, Y., Shi, H., ... & Zhou, C. (2024). Reconciled estimation of Antarctic ice sheet mass balance and contribution to global sea level change from 1996 to 2021. *Science China Earth Sciences*, *67*(11), 3562–3578. https://doi.org/10.1007/s11430-023-1394-5

Lim, E.-P., Hendon, H. H., Arblaster, J. M., Delage, F., Nguyen, H., Min, S.-K., & Wheeler, M. C. (2016). The impact of the Southern Annular Mode on future changes in Southern Hemisphere rainfall. *Geophysical Research Letters*, *43*(13), 7160–7167. https://doi.org/10.1002/2016GL069453

Naakka, T., Nygerd, T., & Vihma, T. (2021). Air moisture climatology and related physical processes in the Antarctic on the basis of ERA5 reanalysis. *Journal of Climate*, *34*(11), 4463–4480. https://doi.org/10.1175/JCLI-D-20-0798.1

Orr, A., Deb, P., Clem, K. R., Gilbert, E., Bromwich, D. H., Boberg, F., Colwell, S., Hansen, N., Lazzara, M. A., Mooney, P. A., Mottram, R., Niwano, M., Phillips, T., Pishniak, D., Reijmer, C. H., van de Berg, W. J., Webster, S., & Zou, X. (2023). Characteristics of surface "Melt Potential" over Antarctic Ice Shelves based on regional atmospheric model simulations of summer air temperature extremes from 1979/80 to 2018/19. *Journal of Climate*, *36*(10), 3357–3383. https://doi.org/10.1175/JCLI-D-22-0386.1

Orr, A., Marshall, G. J., Hunt, J. C. R., Sommeria, J., Wang, C.-G., van Lipzig, N. P. M., Cresswell, D., & King, J. C. (2008). Characteristics of summer airflow over the Antarctic Peninsula in response to recent strengthening of Westerly Circumpolar Winds. *Journal of the Atmospheric Sciences*, *65*(4), 1396–1413. https://doi.org/10.1175/2007JAS2498.1

Press, A. J., & Constable, A. J. (2022). Conservation law in Antarctica and the Southern Ocean: The Antarctic Treaty System, conservation, and environmental protection. *Australian Journal of International Affairs*, *76*(3), 305–323. https://doi.org/10.1080/10357718.2022.2057920

Pysarenko, L., Pishniak, D., & Savenets, M. (2023). Variability of extreme precipitation in West Antarctica and its response to the Amundsen Sea Low changes. *Ukrainian Antarctic Journal*, *21*(2(27), 175–189. https://doi.org/10.33275/1727-7485.2.2023.716

Raphael, M. N., Holland, M. M., Landrum, L., & Hobbs, W. R. (2019). Links between the Amundsen Sea Low and sea ice in the Ross Sea: seasonal and interannual relationships. *Climate Dynamics*, *52*(3–4), 2333–2349. https://doi.org/10.1007/s00382-018-4258-4

Raphael, M. N., Marshall, G. J., Turner, J., Fogt, R. L., Schneider, D., Dixon, D. A., Hosking, J. S., Jones, J. M., & Hobbs, W. R. (2016). The Amundsen Sea Low: Variability, change, and impact on Antarctic climate. *Bulletin of the American Meteorological Society*, *97*(1), 111–121. https://doi.org/10.1175/BAMS-D-14-00018.1

Reboita, M. S., Nieto, R., da Rocha, R. P., Drumond, A., Vázquez, M., & Gimeno, L. (2019). Characterization of moisture sources for austral seas and relationship with sea ice concentration. *Atmosphere*, *10*(10), 627. https://doi.org/10.3390/atmos10100627

Roussel, M.-L., Lemonnier, F., Genthon, C., & Krinner, G. (2020). Brief communication: evaluating Antarctic precipitation in ERA5 and CMIP6 against CloudSat observations. *The Cryosphere*, *14*(8), 2715–2727. https://doi.org/10.5194/tc-14-2715-2020

Schlosser, E., Powers, J. G., Duda, M. G., & Manning, K. W. (2011). Interaction between Antarctic sea ice and synoptic activity in the circumpolar trough: implications for ice-core interpretation. *Annals of Glaciology*, *52*(57), 9–17. https://doi.org/10.3189/172756411795931859

Shepherd, A., Ivins, E., Rignot, E., Smith, B., van den Broeke, M., Velicogna, I., Whitehouse, P., Briggs, K., Joughin, I., Krinner, G., Nowicki, S., Payne, T., Scambos, T., Schlegel, N., A, G., Agosta, C., Ahlstrøm, A., Babonis, G., Barletta, V., ... & Wouters, B. (2018). Mass balance of the Antarctic Ice Sheet from 1992 to 2017. *Nature*, *558*, 219–222. https://doi.org/10.1038/s41586-018-0179-y

Siegert, M., Atkinson, A., Banwell, A., Brandon, M., Convey, P., Davies, B., Downie, R., Edwards, T., Hubbard, B., Marshall, G., Rogelj, J., Rumble, J., Stroeve, J., & Vaughan, D. (2019). The Antarctic Peninsula under a 1.5 °C global warming scenario. *Frontiers in Environmental Science*, *7*, 102. https://doi.org/10.3389/fenvs.2019.00102

Tetzner, D., Thomas, E., & Allen, C. (2019). A validation of ERA5 reanalysis data in the Southern Antarctic Peninsula—Ellsworth Land Region, and its implications for ice core studies. *Geosciences*, *9*(7), 289. https://doi.org/10.3390/geosciences9070289

Tobin, D. M., Kumjian, M. R., Oue, M., & Kollias, P. (2023). Refreezing of partially melted hydrometeors: Polarimetric radar observations and microphysical model simulations. *Journal of the Atmospheric Sciences*, *80*(3), 725–741. https://doi.org/10.1175/JAS-D-22-0174.1

Turner, J., Harangozo, S. A., Marshall, G. J., King, J. C., & Colwell, S. R. (2002). Anomalous atmospheric circulation over the Weddell Sea, Antarctica during the Austral summer of 2001/02 resulting in extreme sea ice conditions. *Geophysical Research Letters*, *29*(24), 13-1–13-4. https://doi.org/10.1029/2002GL015565

Turner, J., Leonard, S., Lachlan-Cope, T., & Marshall, G. J. (1998). Understanding Antarctic Peninsula precipitation distribution and variability using a numerical weather prediction model. *Annals of Glaciology*, 27, 591–596. https://doi.org/10.3189/1998AoG27-1-591-596

Turner, J., Lu, H., King, J., Marshall, G. J., Phillips, T., Bannister, D., & Colwell, S. (2021). Extreme temperatures in the Antarctic. *Journal of Climate*, *34*(7), 2653–2668. https://doi.org/10.1175/JCLI-D-20-0538.1

Turner, K. A., Naughten, K. A., Holland, P. R., & Naveira Garabato, A. C. (2025). Modeled centennial ocean warming in the Amundsen Sea driven by thermodynamic atmospheric changes, not winds. *Geophysical Research Letters*, *52*(14), e2024GL112287. https://doi.org/10.1029/2024GL112287

Vignon, É., Roussel, M.-L., Gorodetskaya, I. V., Genthon, C., & Berne, A. (2021). Present and future of rainfall in Antarctica. *Geophysical Research Letters*, *48*(8), e2020GL092281. https://doi.org/10.1029/2020GL092281

Višnjević, V., Moss, G., Henry, A. C. J., Wild, C. T., Steinhage, D., & Drews, R. (2025). Mapping the composition of Antarctic Ice Shelves as a metric for their susceptibility to future climate change. *Geophysical Research*

Letters, *52*(12), e2024GL112585. https://doi.org/10.1029/2024GL112585

Wang, S., Li, G.-C., Zhang, Z.-H., Zhang, W.-Q., Wang, X., Chen, D., Chen, W., & Ding, M.-H. (2025). Recent warming trends in Antarctica revealed by multiple reanalysis. *Advances in Climate Change Research*, *16*(3), 447–459. https://doi.org/10.1016/j.accre.2025.03.003

Wang, S., Liu, G., Ding, M., Chen, W., Zhang, W., & Lv, J. (2021). Potential mechanisms governing the variation in rain/snow frequency over the northern Antarctic Peninsula during austral summer. *Atmospheric Research*, *263*, 105811. https://doi.org/10.1016/j.atmosres.2021.105811

Wille, J. D., Favier, V., Gorodetskaya, I. V., Agosta, C., Kittel, C., Beeman, J. C., Jourdain, N. C., Lenaerts, J. T. M., & Codron, F. (2021). Antarctic atmospheric river climatology and precipitation impacts. *Journal of Geophysical Research: Atmospheres*, *126*(8), e2020JD033788. https://doi.org/10.1029/2020JD033788

Worster, M. G. (2014). Dynamics of marine ice sheets. *Procedia IUTAM*, *10*, 263–272. https://doi.org/10.1016/j.piutam.2014.01.022

Zhang, C., Zhang, J., & Wu, Q. (2021). Antarctic Peninsula regional circulation and its impact on the surface melt of Larsen C Ice Shelf. *Journal of Climate*, *34*(17), 7297–7309. https://doi.org/10.1175/JCLI-D-20- 1002.1

Received: 26 August 2025
Accepted: 3 November 2025

Зв'язок між мінливістю погоди та кліматичним диполем атмосферного тиску в Антарктичному регіоні морів Амундсена, Беллінсгаузена та Ведделла

Лариса Писаренко[1, 2, *], Михайло Савенець[1], Денис Пішняк[2]

[1] Український гідрометеорологічний інститут Державної служби України з надзвичайних ситуацій та Національної академії наук України, м. Київ, 03028, Україна
[2] Державна установа Національний антарктичний науковий центр МОН України, м. Київ, 01601, Україна

*** Автор для кореспонденції:** lolinal@ukr.net, larpys@uhmi.org.ua

Реферат. Кліматичний диполь атмосферного тиску, що сформований полем низького тиску моря Амундсена (ТМА) та областю високого тиску на схід від Антарктичного півострова (АП), є одним із головних чинників погодної мінливості у Західній Антарктиді та регіоні АП. В умовах поточних кліматичних змін роль цієї конфігурації тиску часто залишається невизначеною. Використовуючи дані реаналізу ERA5 за 1991–2022 рр., ми дослідили відгук різного фазового стану опадів та приземних метеорологічних полів на варіації кліматичного диполя тиску. Посилення та східне зміщення ТМА зумовлювали зростання кількості снігопадів над морями Амундсена і Беллінсгаузена, особливо поблизу самого центру низького тиску, тоді як опади біля АП мали тенденцію переходити з твердих у змішані або рідкі фази. Посилення високого тиску над західною частиною моря Ведделла, особливо у випадках його зміщення ближче до АП, було пов'язане із загальним зменшенням кількості опадів, проте супроводжувалося частішими випадками льодяного дощу та крижаної крупи над північно-східною частиною АП. Ці зв'язки мали виражену просторову неоднорідність і чітку сезонність. Приземні метеорологічні параметри загалом демонстрували слабшу реакцію на диполь тиску, ніж опади. Поглиблений ТМА зазвичай призводив до зниження приземної температури повітря та температури точки роси над східною частиною моря Беллінсгаузена, тоді як його східне зміщення призводило до тепліших умов у межах досліджуваної області. Гребінь високого тиску, розташованого на схід від АП, істотно впливав на термічний режим над морем Ведделла та Землі Королеви Мод і був пов'язаний з інтенсифікацією південних і західних вітрів у південній частині АП. Загалом, це дослідження розширює розуміння того, як приземні метеорологічні умови у Західній Антарктиді реагують на варіації регіонального диполя атмосферного тиску.

Ключові слова: Антарктида, атмосферний тиск, метеорологічні характеристики, опади, поле низького тиску моря Амундсена, реаналіз

APPENDIX

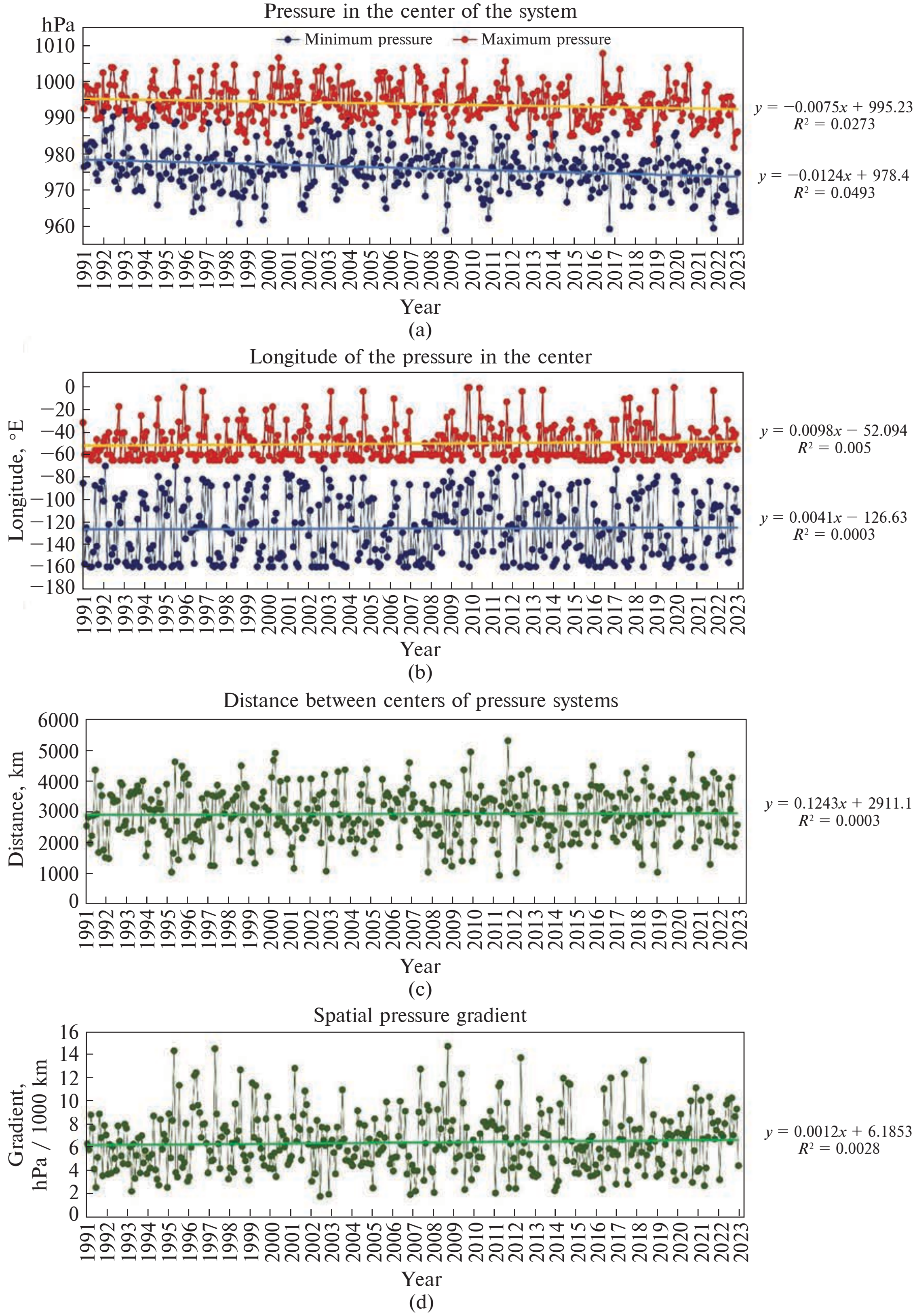

Figure A1. Time series of the monthly values and linear trends for pressure in the centers (a), their longitudes (b), distance between centers of the pressure systems (c) and spatial pressure gradient (d) for 1991–2022

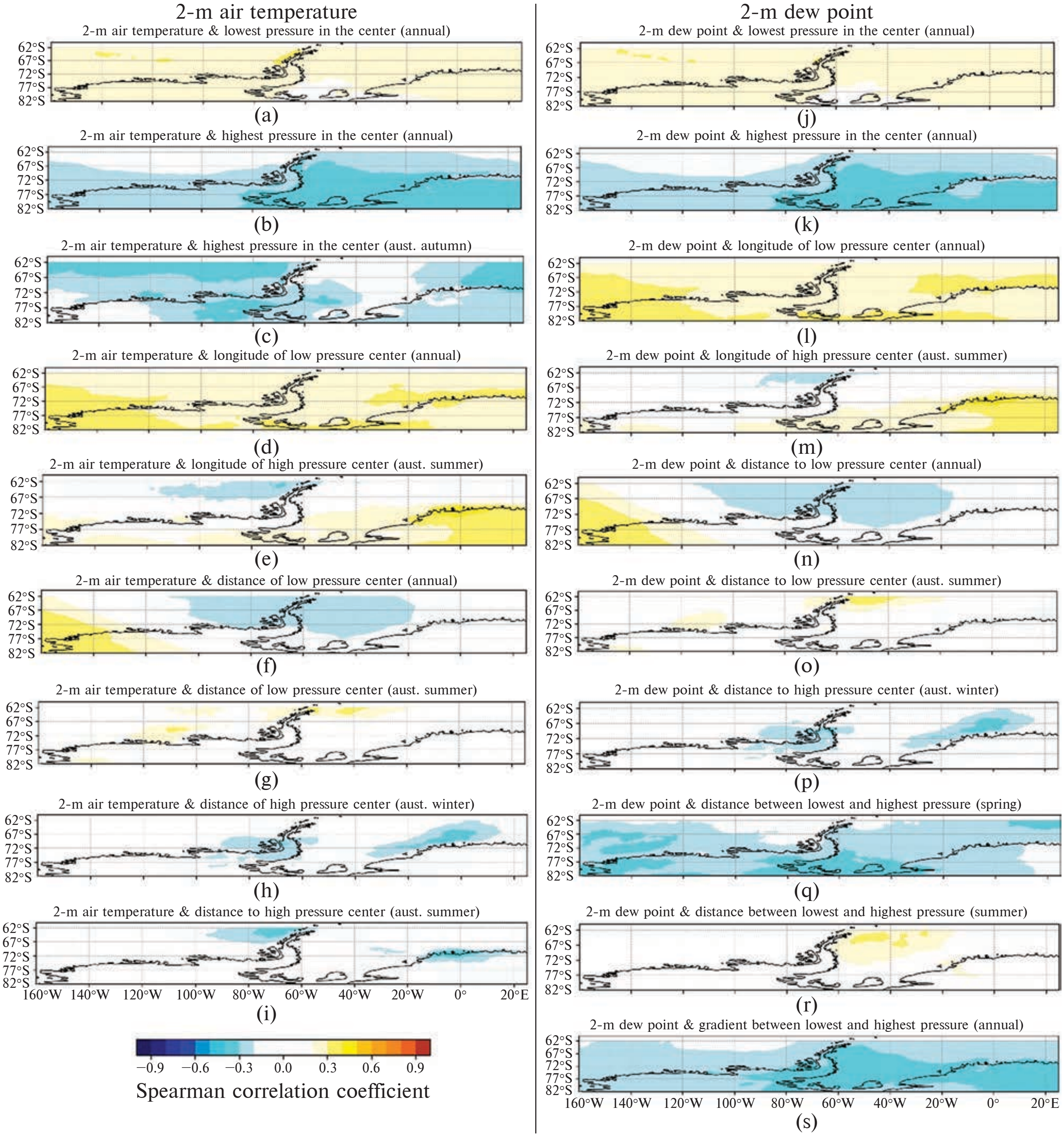

Figure A2. Spatial distributions of the Spearman correlation coefficient between the pressure parameters and 2-m air temperature (a–i) and dew point (j–s)

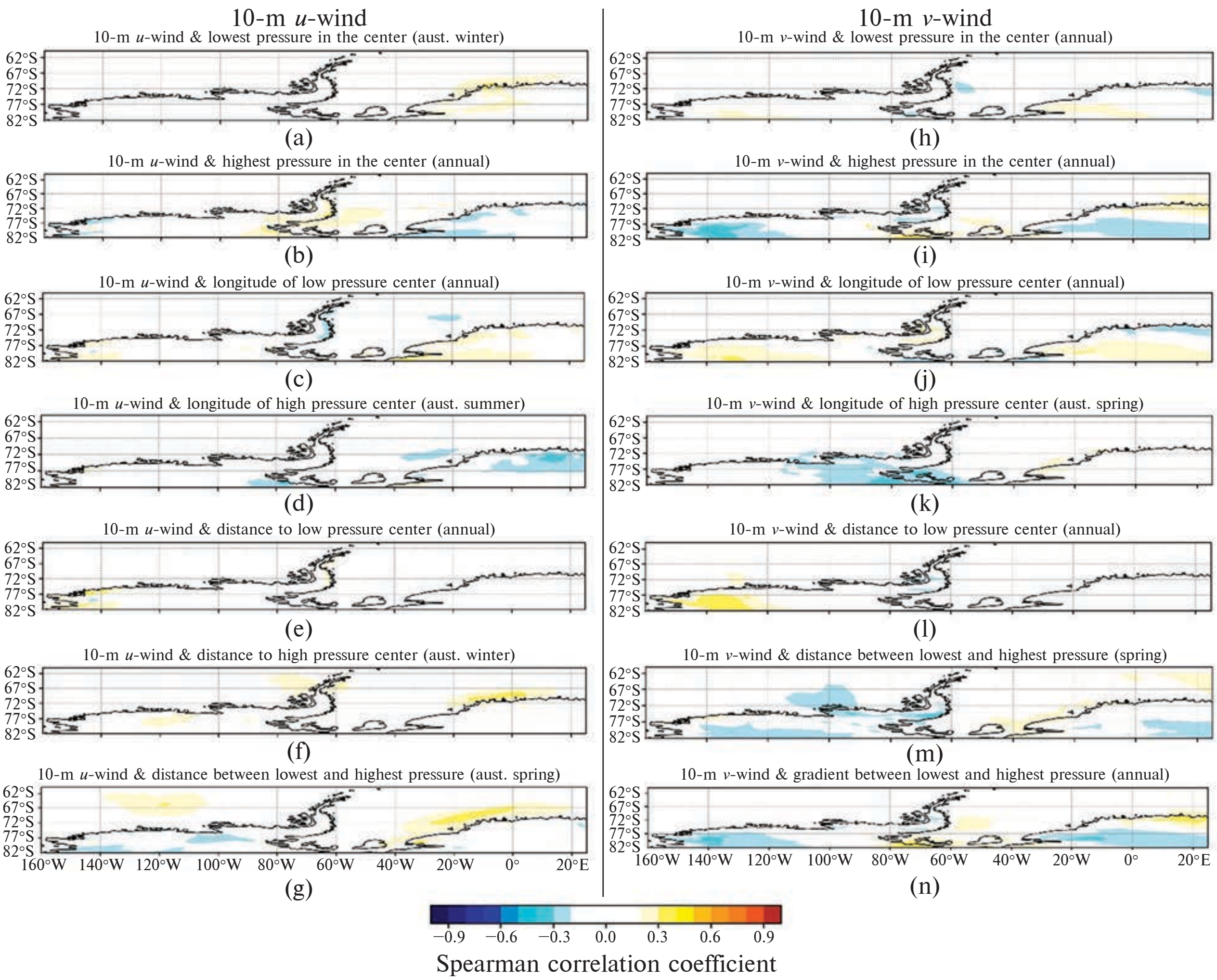

Figure A3. Spatial distribution of the Spearman correlation coefficient between pressure parameters and the 10-m *u*- (a—g) and *v*- (h—n) components of wind